文章编号：0258-7106（2022）04-0770-19 Doi: 10. 16111/j. 0258-7106. 2022. 04. 007

# 滇东北松梁铅锌矿床成矿物质来源：来自S、Pb、Zn同位素的证据*

伊丽娜[1]，李 波[1**]，王新富[1]，韩润生[1]，唐 果[2]，张羽洋[3]

（1 昆明理工大学 国土资源工程学院/有色金属矿产地质调查中心西南地质调查所，云南 昆明 650093；2 中国有色金属工业昆明勘察设计研究院有限公司，云南 昆明 650051；3 贵州省有色金属和核工业地质勘查局，贵州 贵阳 550002）

**摘 要** 川滇黔铅锌多金属成矿域内，碳酸盐岩容矿的热液铅锌矿床多达400个。松梁铅锌矿床地处滇东北与川东南的交接处，位于川滇黔铅锌多金属成矿域的核心部位；铅锌矿体赋存于震旦系灯影组白云岩内，矿体产出明显受断裂控制；矿石矿物组成简单，主要由闪锌矿、方铅矿和黄铁矿组成。文章重点研究了松梁铅锌矿床硫化物的S、Pb、Zn同位素组成，进而探讨了其成矿物质来源及矿床成因。研究表明，松梁铅锌矿床的硫化物$\delta^{34}S_{CDT}$值在+4.6‰~+13.7‰之间，平均值为+10.5‰，显示硫来源于赋矿围岩，为震旦系灯影组硫酸盐经TSR的产物；硫化物的Pb同位素比值为$^{206}Pb/^{204}Pb$=18.158~18.513、$^{207}Pb/^{204}Pb$=15.633~15.895、$^{208}Pb/^{204}Pb$=38.096~38.786，反映成矿物质为壳源铅，源自震旦系灯影组白云岩与结晶基底的混合；闪锌矿的$\delta^{66}Zn$为−0.126‰~+0.082‰，揭示成矿物质可能源自震旦系灯影组碳酸盐岩和结晶基底的混合。松梁铅锌矿床为后生碳酸盐岩容矿型铅锌矿床。

**关键词** 地球化学；硫、铅、锌同位素；成矿物质来源；矿床成因；松梁铅锌矿床；滇东北

**中图分类号**：P618.42；P618.43 **文献标志码**：A

# Sources of metallogenic materials of Songliang lead-zinc deposit in northeastern Yunnan, China: Evidence from S, Pb and Zn isotopes

YI LiNa[1], LI Bo[1], WANG XinFu[1], HAN RunSheng[1], TANG Guo[2] and ZHANG YuYang[3]

(1 Faculty of Land Resource Engineering, Kunming University of Science and Technology / Southwest Institute of Geological Survey, Geological Survey Center for Nonferrous Metals Resources, Kunming 650093, Yunnan, China; 2 China Nonferrous Metals Industry Kunming Survey and Design Institute Co. LTD., Kunming 650051, Yunnan, China; 3 Guizhou Bureau of Geological Exploration for Nonferrous Metals and Nuclear Industry, Guiyang 550002, Guizhou, China)

**Abstract**

There are as many as 400 hydrothermal Pb-Zn deposits hosted by carbonate rocks in Sichuan-Yunnan-Guizhou Pb-Zn polymetallic metallogenic province. The Songliang Pb-Zn deposit is located at the intersection of northeast Yunnan and southeast Sichuan, where is the core of SYG Pb-Zn polymetallic metallogenic province. The Pb-Zn ore bodies of the Songliang deposit occur in the dolomite of the Sinian Dengying Formation, and its occurrence is controlled by faults obviously. Sulfide minerals are mainly composed of sphalerite, galena and pyrite with simple composition. This paper focused on the composition of S, Pb and Zn isotopes, and then discussed the source of ore-forming materials and the genesis of the Songliang deposit. The analytical results show that the

* 本文得到云南省万人计划青年拔尖人才项目（编号：YNWR-QNBJ-2018-093）、国家自然科学基金项目（编号：41862007）和昆明理工大学重点学科建设项目（编号：14078384）联合资助

第一作者简介 伊丽娜，女，1997年生，硕士研究生，矿物学、岩石学、矿床学专业。Email：yilina1997@163.com

** 通讯作者 李 波，男，1981年生，教授，博士，从事矿床学及构造地球化学研究。Email：libo8105@qq.com

收稿日期 2022-01-29；改回日期 2022-06-23。张绮玲编辑。

$\delta^{34}S_{CDT}$ values of sulfides from the Songliang deposit ranged from +4.6‰ to +13.7‰, with an average of +10.5‰, indicating that the sulfur was derived from host rocks and was the product of TSR of sulphates in the Sinian Dengying Formation. The Pb isotope ratios of sulfide samples were relatively uniform and $^{206}Pb/^{204}Pb$=18.158~18.513, $^{207}Pb/^{204}Pb$=15.633~15.895, $^{208}Pb/^{204}Pb$=38.096~38.786, reflecting a crustal source which is the mixture of dolomite in the Sinian Dengying Formation and crystalline basement. The $\delta^{66}Zn$ of sphalerite is in the range of −0.126 ‰ to +0.082 ‰, which indicates that the ore-forming materials are derived from the mixture of the Sinian Dengying Formation carbonate rocks and basement rocks in the Kunyang and Huili Group. The Songliang Pb-Zn deposit was an epigenetic Pb-Zn deposit hosted by carbonate rocks.

**Key words:** geochemistry, sulfur-lead-zinc isotopes, source of ore-forming materials, genesis of deposit, Songliang Pb-Zn deposit, northeastern Yunnan Province

川滇黔铅锌成矿域位于四川-云南-贵州三省的交界地区,地处扬子板块西南缘(Zhou et al., 2014a)(图 1),属华南低温成矿域的一部分(Hu et al., 2017; Wu et al., 2021)。成矿域内分布有超过400个铅锌矿床(点)(Li et al., 2018; Zhang et al., 2019a; 2019b; Tan et al., 2019; Zhu et al., 2020),为中国铅、锌、银、锗等金属的重要产地(He Y F et al., 2020; He Z W et al., 2021),已探明铅锌储量高达 260 Mt,铅锌品位达10%,甚至个别矿床达到30%(Zhou et al., 2015)。成矿域内有3个超大型铅锌矿床,即滇东北的会泽铅锌矿床、毛坪铅锌矿床以及黔西北的猪拱塘铅锌矿床(Wei et al., 2021a)。对该成矿域内铅锌矿床的成因一直争议较大,主要有岩浆-热液成因(谢家荣, 1941)、沉积成因(张位及, 1984)、沉积-改造成因(廖文, 1984)等,是否属MVT型铅锌矿床成为争议的焦点。近十年来的研究成果显示,川滇黔成矿域内绝大多数铅锌矿床的后生特征明显,可与MVT型铅锌矿床类比,在矿化类型、赋矿地层岩性、矿物组合、围岩蚀变等方面与典型MVT型矿床基本一致(张长青, 2005; 吴越, 2013)。也有学者认为,川滇黔成矿域内铅锌矿体品位普遍比典型MVT型矿床的高,部分矿床在矿床地质特征、成矿物质来源、成矿流体特征等方面均与典型MVT型铅锌矿床有明显区别,如铅锌矿体呈巨厚脉状产出的会泽超大型矿床,是世界上品位最高的铅锌矿床之一(黄智龙等, 2004; 韩润生等,2006)。对此,有学者提出了新的成因类型,如韩润生等(2012)提出会泽矿床为HZT(会泽型)铅锌矿床,Zhou 等(2018) 提出富乐矿床为SYG(川滇黔型)铅锌矿床。

松梁铅锌矿床位于滇东北昭通市巧家县境内,为小型铅锌矿床(李波等,2014)。前人研究了矿床地质特征、控矿构造、构造地球化学,开展了找矿预测等(李波, 2008;2010;李波等, 2014),尚缺乏矿床地球化学研究资料,导致其成矿物质来源和矿床成因不清。对于川滇黔成矿域内铅锌矿床的成矿物质,多认为源自基底地层、赋矿围岩或峨眉山玄武岩(黄智龙等,2001;李文博等, 2006),松梁铅锌矿床的成矿物质来源和矿床成因,成为亟待解决的科学问题。

同位素示踪已成为研究成矿物质来源及矿床成因的强有力手段(Zhou et al., 2013a; 李延河, 2020)。硫同位素在自然界的分馏变化范围大,是了解成岩成矿过程的有效示踪剂,用以确定硫源、限制热液的性质(Maanijou et al., 2020; Wei et al., 2020; Rddad, 2021)。铅同位素研究是基于各地质储库的铅同位素组成端员值、边界值,追踪不同地质储库对矿床成矿Pb物质组成的贡献(孙卫东等,2012)。锌同位素作为非传统稳定同位素,已被广泛应用于宇宙化学、地球化学和生物化学等领域(王中伟等, 2015)。得益于高精度质谱技术的快速发展,鉴别锌同位素等重元素同位素的微小分馏成为现实。Zn元素本身相对于其他成矿元素具有较高丰度(Zhu et al., 2020),锌同位素已广泛应用于示踪铅锌矿床的Zn来源、分析成矿元素的沉淀机制和矿床成因等(Pašava et al., 2014; Zhou et al., 2014a; 2014b; Zhu et al., 2018; 2020)。本文在前人研究成果的基础上,分析了松梁铅锌矿床的硫、铅和锌同位素组成,借以示踪成矿物质来源,进而分析其矿床成因,以丰富川滇黔铅锌成矿域的成矿理论。

## 1　区域地质背景

扬子板块西南缘与三江褶皱带以深大断裂(金沙江-红河断裂;图 1)为界,地层具有“双基双盖”结构,即太古宙—中元古代形成的结晶基底、新元古代形成的褶皱基底、早震旦世的海相不连续沉积盖层和晚震旦世—晚古生代的连续沉积盖层,构造变形以断

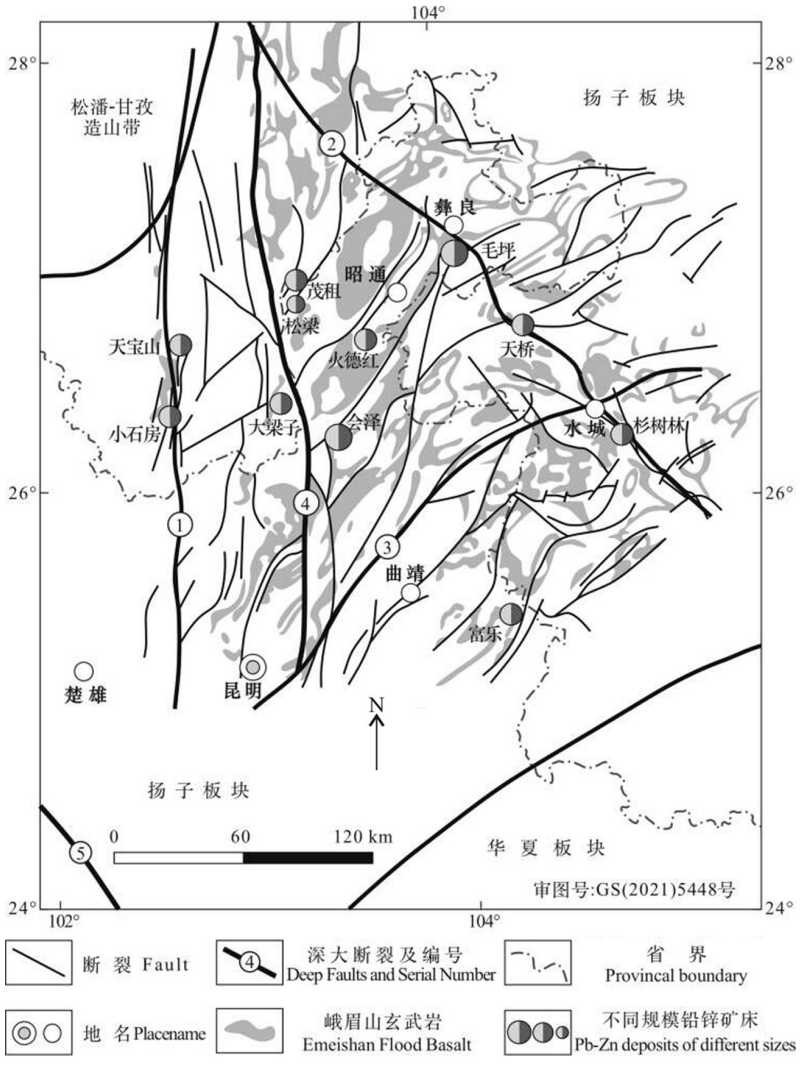


图1 川滇黔Pb-Zn成矿域矿产分布(据Zhou et al., 2018a修改)

深大断裂:①—安宁河-绿汁江断裂;②—康定-彝良-水城断裂;③—弥勒-师宗-水城断裂;④—小江断裂;⑤—金沙江-红河断裂

Fig. 1 Mineral deposits distribution in the Sichuan-Yunnan-Guizhou Pb-Zn metallogenic province (modified from Zhou et al., 2018a)

Deep fault: ①—Anninghe-Luzhijiang fault; ②—Kangding-Yiliang-Shuicheng fault; ③—Mile-Shizong-Shuicheng fault; ④—Xiaojiang fault; ⑤—Jinshajiang-Honghe fault

裂发育为主要特征(张长青等, 2005; 孔志岗等,2018)。

川滇黔铅锌成矿域地处环太平洋构造域和特提斯构造域的结合部位,其东南与华夏板块相靠,西南与三江褶皱系相邻,北与松潘甘孜造山带相接。成矿域大致呈“三角区”,以SN向的安宁河-绿汁江断裂、NW向的康定-彝良-水城断裂和NE向的弥勒-师宗-水城断裂为构造格架(图1)。

滇东北地区为川滇黔铅锌多金属成矿域的重要组成部分,地处小江深断裂东侧(图1),多期次构造运动强烈(张长青, 2005; 李波, 2010)。区内已发现大量以碳酸盐岩为容矿围岩的铅锌(银锗)矿床,具备优越的成矿地质条件(Zhou et al., 2014b; Xu et al., 2020)。

太古宙至古元古代,扬子板块西南缘形成结晶基底;中新元古代开始形成褶皱基底,该褶皱基底主要为一套中-低级变质岩,新元古代震旦纪形成了一套以碳酸盐岩为主的沉积地层。寒武纪—二叠纪期间,川滇黔成矿域大部分地区接受沉积,但部分地区缺失上奥陶统至石炭系。海西运动晚期,地幔物质不断上涌,大量基性玄武岩浆在四川、云南和贵州等地大面积喷溢,形成了峨眉山大火成岩省(260~254 Ma; Shellnutt et al., 2020);面积超过30多万km$^2$,平均厚度为607 m,最大厚度>3000 m,其形成时代、火山

作用持续时间、与Guadalupian生物大灭绝的关联、成因机制等被广泛研究(黄智龙等, 2001; He et al., 2014; Shellnutt, 2014; Huang et al., 2019; 王婕等, 2019; Fu et al., 2021)。晚二叠世末期至早-中三叠世,该区又经历了一次大范围海侵事件,上扬子古陆发展为上扬子陆表海,部分地区接受碎屑岩沉积。印支运动近水平的挤压作用及其派生的NNW-SSE向的拉张作用,导致滇东北地区形成了规模不等的近SN向断裂带。晚三叠世,北特提斯边缘盆关闭,攀西裂谷盆地转化为内陆凹陷盆地,该时期为川滇黔铅锌成矿域的大规模成矿时期(张长青等, 2005)。

## 2　矿床地质

松梁铅锌矿床位于小江断裂东侧、莲峰-巧家断裂东南侧(李波, 2008),矿区内出露地层为上震旦统灯影组($Z_2dn$)、下寒武统筇竹寺组($\in_1q$)及下奥陶统巧家组($O_1q$)(图2)。

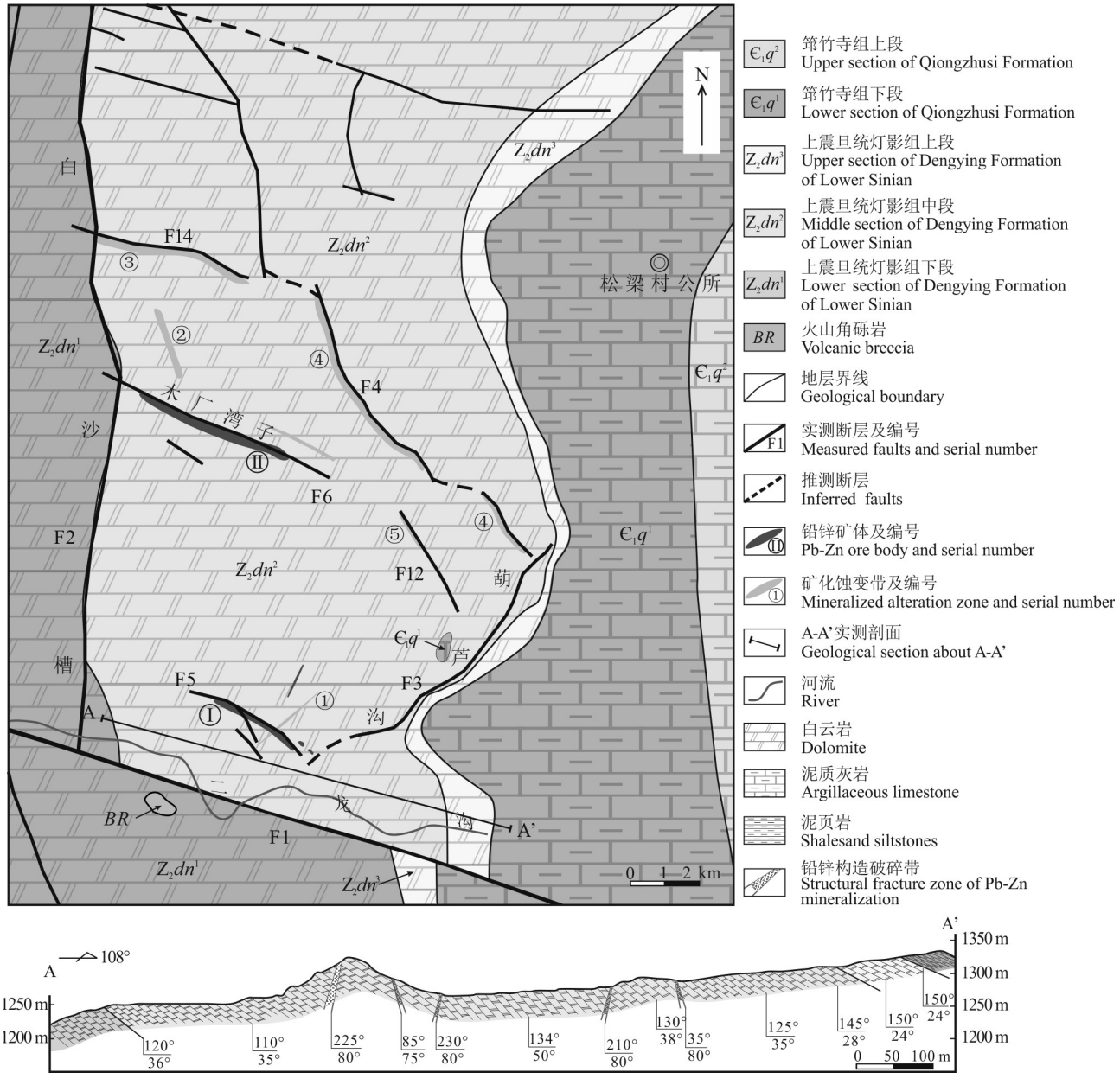


图2　松梁Pb-Zn矿床地质简图及A-A'剖面图(据李波,2010)

Fig. 2　Simplified geologic map of the Songliang Pb-Zn deposit and A-A' cross section through the deposit (after Li, 2010)

灯影组($Z_2dn$)广泛分布于矿区中-西部,呈近SN向展布,为一套海侵系列的碳酸盐岩;根据岩性、岩石结构及生物组合特征,可分为3段:灯影组下段($Z_2dn^1$)为灰白色-深灰色厚层状白云岩夹白云质灰岩,偶含硅质结核;灯影组中段($Z_2dn^2$)为富含硅质条带的浅灰色中-厚层状云岩,中上部为灰白色厚层块状白云岩,具硅质结核或硅质条带,下部为灰色-灰白色厚层块状云岩,底部为紫红色含钙云质岩、砂岩和灰绿色含白云质泥质灰岩及硅质岩;灯影组上段($Z_2dn^3$)为乳白色、浅灰色含磷白云岩,夹黑色条带状磷块岩及硅质结核层。其中灯影组中、上段($Z_2dn^2$、$Z_2dn^3$)白云岩是该区主要的赋矿地层。筇竹寺组($\in_1q$)分布于矿区东部及南部,其下段($\in_1q^1$)为灰色至褐黑色细粒泥质砂岩,上段($\in_1q^2$)主要为紫红色、黄色页岩与灰色、紫红色泥质灰岩互层,夹泥质砂岩。巧家组($O_1q$)出露于筇竹寺组东部,主要为灰色-深灰色中-厚层状泥质灰岩、生物碎屑灰岩等,夹灰色钙质砂岩、页岩、泥砂质灰岩。

围岩蚀变简单,主要有白云石化、硅化、方解石化、黄铁矿化和少量重晶石化,反映出中、低温热液成矿特点。其中白云石化较普遍,且围岩褪色现象明显,局部地段形成灰白色粉末,被当地老乡称为“炮灰”,为重要的找矿标志之一。

松梁铅锌矿床目前已发现2个铅锌矿体、4条铅锌矿化蚀变带。矿体呈脉状、透镜体状产出,其形态特征和空间展布明显受断裂控制(图2)。矿区断裂发育,可分为NW向、NE向和近SN向3组,矿体及矿化带均产出于NW向断裂及其与NE向层间断裂的交汇处。NW向断裂以F1(二龙沟断裂)和F5(二龙沟北坡断裂)、F6(白沙槽-木厂湾子断裂)为代表;总体走向NW50°~70°,倾向NE,倾角较陡(>62°),局部反倾;F5和F6严格控制着Ⅰ号和Ⅱ号矿体的空间产出,为该矿床的主要容矿构造。NE向断裂组以F3(葫芦沟断裂)为代表,多为层间断裂,总体走向NE20°~70°,倾向SE或NW,倾角约45°。近SN向断裂以F2(白沙槽断裂)为主。

矿石中矿物组成简单,金属矿物主要由闪锌矿、方铅矿、黄铁矿等硫化物和菱锌矿、锌矾等氧化物组成,非金属矿物主要为方解石、白云石及少量石英。矿石结构主要为压碎结构、交代结构、溶蚀结构、交代残余结构、固溶体分离结构、共边结构、他形填隙结构等(图3e~m)。矿石构造主要有斑点状和斑杂状构造、细脉状和网脉状构造、条带状构造、块状构造、角砾状构造等(图3a~d)。

依据矿石组构特征、矿物共生组合以及矿脉之间的穿插关系,松梁铅锌矿床的形成过程可划分为沉积-成岩期、热液成矿期和表生氧化期。其中,热液成矿期又可分为3个成矿阶段:(Ⅰ)闪锌矿-黄铁矿阶段、(Ⅱ)闪锌矿-方铅矿-石英阶段和(Ⅲ)闪锌矿-方铅矿-黄铁矿-方解石阶段(图4)。黄铁矿的生成贯穿于整个成矿过程,闪锌矿和方铅矿主要形成于Ⅱ、Ⅲ阶段。

## 3 样品采集及测试方法

本文采集了松梁铅锌矿床不同部位的典型矿石标本,在手标本描述和显微镜下鉴定的基础上,分别挑选闪锌矿、方铅矿和黄铁矿单矿物样品,纯度在99.99%以上。硫同位素(闪锌矿19件、方铅矿6件、黄铁矿2件)测试在广州澳实公司(ALS Scandinavia AB)同位素实验室和中国科学院矿床地球化学国家重点实验室进行。铅同位素(闪锌矿9件、方铅矿5件、黄铁矿2件)和锌同位素(闪锌矿6件)测试在广州澳实公司(ALS Scandinavia AB)同位素实验室进行。

硫同位素测定使用元素分析仪-气体同位素质谱(EA-IRMS)测$^{34}S/^{32}S$,数据采用相对国际硫同位素标准CDT(Canyon Diablo Troilite)值表示,标准物质选用NBS127,RSD<0.03%。锌同位素采用$HNO_3$+HCl+HF消解相结合的方法制备,在离子交换分离后得出分析结果,锌同位素比值的δ值($\delta^{66/64}Zn$及$\delta^{68/64}Zn$)基于IRMM-3702CRM标准化,标准偏差(σ)是从两次连续的独立测试结果中得出,以反映数据的精密度。

## 4 测试结果

松梁铅锌矿床的硫化物(闪锌矿、方铅矿、黄铁矿)硫同位素组成见表1,$\delta^{34}S_{CDT}$值变化范围介于+4.6‰~+13.7‰,均值+10.5‰($n$=27)。闪锌矿、方铅矿、黄铁矿的$\delta^{34}S_{CDT}$有所差异,闪锌矿$\delta^{34}S_{CDT}$介于+5.5‰~+13.7‰,均值+11.0‰($n$=19);方铅矿的$\delta^{34}S$值变化范围较窄,且略低于闪锌矿,其范围为+9.1‰~+11.0‰,均值+10.2‰($n$=6);黄铁矿只有2件,$\delta^{34}S$值为+4.6‰和+9.3‰。松梁铅锌矿床的$\delta^{34}S$值以正值且富重硫为特征(图5a)。

松梁铅锌矿床的硫化物铅同位素组成见表2。闪锌矿$^{206}Pb/^{204}Pb$比值介于18.158~18.513,均值

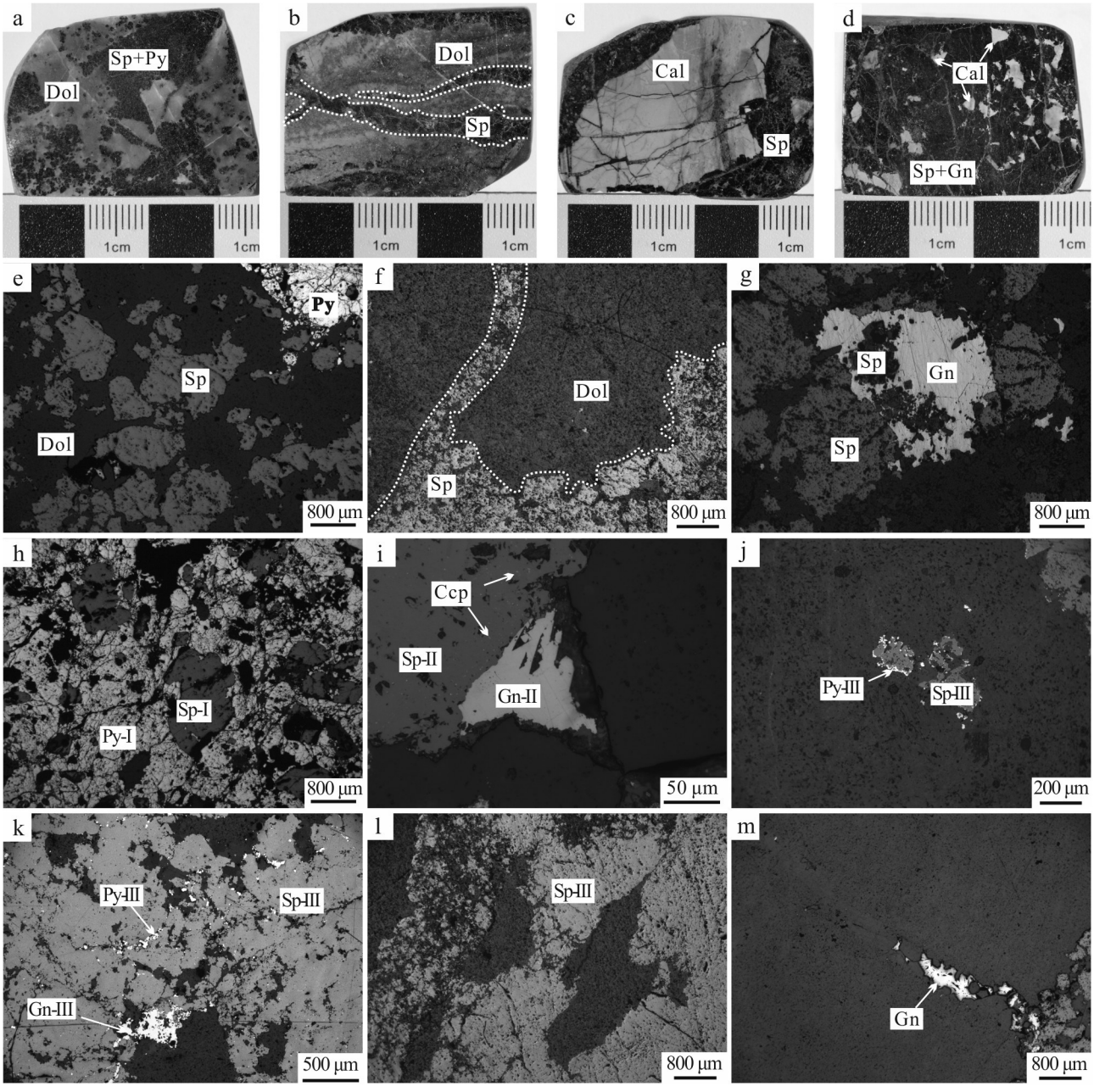


图 3　松梁铅锌矿床的矿石结构构造照片

a. 斑杂状构造;b. 细脉状构造,闪锌矿呈脉状穿插于硅质条带状白云岩内;c. 网脉状构造,闪锌矿细脉交织成不规则网脉状;d. 块状构造、角砾状构造,闪锌矿中含不规则状、棱角状方解石角砾;e. 压碎结构、交代结构,早期碎裂状黄铁矿及不规则粒状闪锌矿交代围岩;f. 细脉状构造、交代结构,细脉状闪锌矿充填交代围岩,与围岩界线模糊;g. 溶蚀结构、交代残余结构,方铅矿沿闪锌矿的边缘及裂隙交代溶蚀闪锌矿,可见一些岛屿状和不规则状闪锌矿残余体;h. 压碎结构、交代结构,自形 . 他形晶黄铁矿呈压碎结构,闪锌矿沿黄铁矿裂隙充填,并交代黄铁矿;i. 固溶体分离结构、共边结构,方铅矿与闪锌矿共生,呈共边结构,黄铜矿呈乳滴状分布在闪锌矿内部;j. 交代结构,黄铁矿沿闪锌矿颗粒周边进行交代;k. 交代结构,不规则状、细脉状方铅矿交代闪锌矿,黄铁矿沿闪锌矿裂隙充填并交代闪锌矿;l. 溶蚀结构,闪锌矿溶蚀交代脉石矿物;m. 填隙结构,他形晶方铅矿填充于石英脉与白云石矿物间孔隙

Sp—闪锌矿;Gn—方铅矿;Py—黄铁矿;Ccp—黄铜矿;Dol—白云石;Q—石英

Fig. 3　Ore texture and structure of the Songliang Pb-Zn deposit

a. Patchy structure; b. Veined and banded structure, veined sphalerite are interspersed in banded siliceous dolomite; c. Stockwork structure, an irregular stockwork of intersecting sphalerite veins; d. Massive and brecciated structure, irregular and brecciated calcite in sphalerite; e. Crushed and metasomatic texture, early crushed pyrite and irregular granular sphalerite replaced the wall rock; f. Veined structure and metasomatic texture, veined sphal-

erite filled and replaced wall rock whose boundary is blurred; g. Dissolution and metasomatic residual texture, galena metasomatically dissolves sphalerite along the edges and fissures of sphalerite, there are some island and irregular sphalerite remains; h. Crushed and metasomatic texture, euhedral &anhedral pyrite with crushed texture, the fissures of the pyrite are filled and replaced by sphalerite; i. Solid solution separation and common edge texture, virus-like chalcopyrite is distributed in the sphalerite, galena and sphalerite are coexisted, showing a common edge texture; j. Metasomatic texture, pyrite metasomatizes around sphalerite grains; k. Metasomatic texture, sphalerite is replaced by irregular and veined galena, and the sphalerite fissures are filled and replaced by pyrite; l. Dissolution texture, gangue minerals are dissolved and replaced by sphalerite; m. Interstitial texture, the cracks of quartz veins and dolomite minerals are filled by anhedral galena

Sp—Sphalerite; Gn—Galena; Py—Pyrite; Ccp—Chalcopyrite; Dol—Dolomite; Q—Quartz

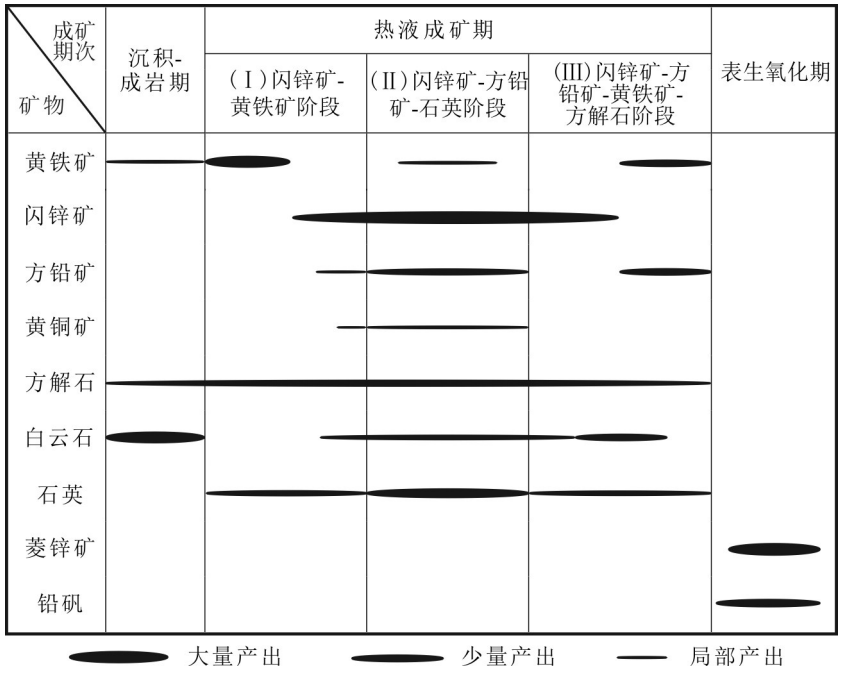


图4 松梁Pb-Zn矿床成矿阶段及矿物生成顺序表

Fig.4 The metallogenic stages and mineral paragenetic sequence of the Songliang Pb-Zn deposit

18.344($n$=9);$^{207}Pb/^{204}Pb$ 比值介于15.633~15.895,均值15.761($n$=9);$^{208}Pb/^{204}Pb$ 比值介于38.096~38.786,均值38.456($n$=9)。方铅矿 $^{206}Pb/^{204}Pb$ 比值介于18.186~18.248,均值18.214($n$=5);$^{207}Pb/^{204}Pb$ 比值介于15.675~15.705,均值15.689($n$=5);$^{208}Pb/^{204}Pb$ 比值介于38.192~38.276,均值38.245($n$=5)。黄铁矿的 $^{206}Pb/^{204}Pb$ 比值为18.237和18.251;$^{207}Pb/^{204}Pb$ 值为15.654和15.672;$^{208}Pb/^{204}Pb$ 值为38.163和38.226。16件硫化物的 $^{206}Pb/^{204}Pb$ 比值介于18.158~18.513,均值18.291;$^{207}Pb/^{204}Pb$ 比值介于15.633~15.895,均值15.727;$^{208}Pb/^{204}Pb$ 比值介于38.096~38.786,均值38.357;测试结果相对集中。μ值变化范围在9.56~10.04之间($n$=16),均值为9.73‰,数据变化范围小。

松梁铅锌矿床的闪锌矿锌同位素组成见表3,6件闪锌矿的 $\delta^{66}Zn_{IRMM-3702}$ 值介于−0.126‰~+0.082‰,均值+0.007‰;$\delta^{68}Zn$ 值介于−0.237‰~+0.155‰,均值+0.015‰。过去锌同位素常用标准物质为JMC-Lyon,但现在已不再适用(Hoefs et al., 2018)。Moeller等(2012)将欧洲标准IRMM-3702校准为新的锌同位素标准,其 $\delta^{66}Zn$ 值相对于JMC-Lyon为0.29‰;为便于对比,本文将所有 $\delta^{66}Zn$ 值统一为IRMM-3702标准。

## 5 讨 论

### 5.1 硫同位素

#### 5.1.1 与川滇黔典型铅锌矿床对比

松梁铅锌矿床硫化物的 $\delta^{34}S$ 值(图5a、b),与同样赋存于震旦系的乌斯河、金沙厂、天宝山、茂租、大梁子矿床的 $\delta^{34}S$ 值存在差异(图5c)。乌斯河铅锌矿床主成矿阶段相对富集重硫同位素($\delta^{34}S$ 值

**表 1　松梁 Pb-Zn 矿床硫化物的硫同位素组成**

**Table 1　Sulfur isotopic compositions of sulfide from the Songliang Pb-Zn deposit**

| 序号 | 样品编号 | 样品名称 | $\delta^{34}S_{CDT}$/‰ | 序号 | 样品编号 | 样品名称 | $\delta^{34}S_{CDT}$/‰ |
|---|---|---|---|---|---|---|---|
| 1 | 07-1-5 | 闪锌矿 | 11.8 | 15 | GQO-24-2 | 闪锌矿 | 5.5 |
| 2 | 07-1-6 | 闪锌矿 | 12.6 | 16 | GQO-24-3 | 闪锌矿 | 6.5 |
| 3 | 6#kengB1 | 闪锌矿 | 13.2 | 17 | QGr231 | 闪锌矿 | 6.3 |
| 4 | 6#kengB2 | 闪锌矿 | 13.7 | 18 | GQ0-24-4 | 闪锌矿 | 6.5 |
| 5 | 6#kengB3 | 闪锌矿 | 11.5 | 19 | GQ0-24-5 | 闪锌矿 | 6.9 |
| 6 | 6#kengB4 | 闪锌矿 | 11.8 | 20 | 6#kengB3 | 方铅矿 | 10.1 |
| 7 | MY6-QGr2 | 闪锌矿 | 11.2 | 21 | MY6-QGH4 | 方铅矿 | 11.0 |
| 8 | MY6-QGH4 | 闪锌矿 | 13.2 | 22 | MY6-QGH8 | 方铅矿 | 10.4 |
| 9 | MY6-QGH5 | 闪锌矿 | 13.4 | 23 | 6#kengB1 | 方铅矿 | 9.7 |
| 10 | MY6-QGH8 | 闪锌矿 | 13.1 | 24 | MY6-QGH14 | 方铅矿 | 9.1 |
| 11 | MY6-QGH12 | 闪锌矿 | 12.9 | 25 | MY6-QGH15 | 方铅矿 | 10.7 |
| 12 | MY6-QGH14 | 闪锌矿 | 13.3 | 26 | 6#kengB3 | 黄铁矿 | 9.3 |
| 13 | MY6-QGH15 | 闪锌矿 | 13.4 | 27 | MY6-QGr2 | 黄铁矿 | 4.6 |
| 14 | MY6-QGR3 | 闪锌矿 | 12.0 | | | | |

为+11.0‰~+23.3‰),为赋矿地层蒸发岩的热化学还原作用的产物(Wei et al., 2020),与松梁铅锌矿床 $\delta^{34}S$ 为正值且富重硫的特征相似;乌斯河铅锌矿床成矿早期的 $\delta^{34}S$ 值较低,基底可能是其潜在硫源(Zhang et al., 2019a)。金沙厂铅锌矿床硫化物中多伴生萤石、石英、重晶石等矿物,与川滇黔地区大部分矿床有所区别,其闪锌矿、方铅矿的 $\delta^{34}S$ 值(+3.6‰~+13.4‰、+3.7‰~+9.0‰)与松梁铅锌矿床闪锌矿、方铅矿的 $\delta^{34}S$ 值(+5.5‰~+13.7‰、+9.1‰~+11.0‰)接近。Bai 等 (2013)研究重晶石的硫同位素组成,认为金沙厂硫化物的还原硫主要与岩浆活动有关,是壳源硫和硫酸盐热化学还原反应(TSR)生成还原硫的混合。天宝山铅锌矿床 $\delta^{34}S$ 值介于 4.24‰~4.87‰,均值 4.59‰,略小于松梁铅锌矿床;何承真等(2016)认为该矿床的硫不完全来源于灯影组白云岩,有少量地幔硫的加入。大梁子和茂租铅锌矿床的硫同位素主要来源于灯影组海相硫酸盐的热化学还原作用(周家喜等, 2012; 王海等, 2018),与松梁铅锌矿床一致,$\delta^{34}S$ 为正值且富集重硫。

5.1.2　硫源

自然界硫源有 3 种:地幔硫、现代海水硫及还原/沉积硫(或称生物硫)。地幔硫的 $\delta^{34}S$ 值接近 0,变化范围在−3‰~+3‰;现代海水硫变化范围很大,$\delta^{34}S$ 值约+20‰,一般认为海相蒸发盐岩的 $\delta^{34}S$ 代表海水硫酸盐的硫同位素值;生物硫则以 $\delta^{34}S$ 负值为特征(陕亮等,2009)。热液矿床中的硫源主要有幔源硫、壳源硫、混合来源硫 3 大类(张云新等,2014; Zhou et al., 2014a; 王云峰等,2016)。其中幔源硫 $\delta^{34}S$ 值接近 0,变化范围小,接近于陨石的硫同位素组成。壳源硫则变化范围很大,地壳物质在岩浆、沉积、变质作用过程中,其硫同位素发生了很大的变化,这就导致了各类地壳岩石的硫同位素组成变化很大;例如海水或海相硫酸盐的硫以富 $^{34}S$ 为特征,生物成因硫则以贫 $^{34}S$、富 $^{32}S$ 为特征。混合来源硫指岩浆在上升侵位过程中混染了地壳物质,导致该类硫同位素组成变化较大。前人研究表明,热液体系还原硫的形成主要通过 2 个过程:硫酸盐热化学还原反应(TSR)和硫酸盐微生物还原反应(BSR),$\Delta^{34}S_{SO_4\text{-}H_2S}$ 最高分别可达 20‰(100~200℃,Machel et al., 1995)和 72‰(< 100℃,Lefticariu et al., 2017)。

松梁铅锌矿床的硫化物主要为闪锌矿、方铅矿和黄铁矿,在这种矿物组合简单的情况下,松梁铅锌矿床主要硫化物 $\delta^{34}S$ 平均值可近似代表成矿热液流体的 $\delta^{34}S_{\sum S\text{-}fluids}$ 值(Ohmoto et al., 1982)。部分共生闪锌矿和方铅矿硫同位素组成呈现出 $\delta^{34}S_{闪锌矿} > \delta^{34}S_{方铅矿}$ 的规律(图 4),表明成矿流体已达到了热力学平衡,松梁铅锌矿床 $\delta^{34}S$ 值(+4.6‰~+13.7‰,均值+10.5‰),显示该矿床还原性硫为壳源硫;相比灯影组硫酸盐 $\delta^{34}S$ 值(+24.0‰~+36.7‰,均值+29.6‰;Goldberg et al., 2005)低 20‰ 左右(图 5b),可以确定松梁矿床硫来源于其赋矿地层(震旦系灯影组硫酸盐),且其 S 还原过程是通过 TSR 进行的,这与茂租、

**表2 松梁Pb-Zn矿床硫化物铅同位素组成**

**Table 2 Lead isotopic compositions of sulfides from the Songliang Pb-Zn deposit**

| 序号 | 样品编号 | 样品名称 | $^{206}Pb/^{204}Pb$ | $^{207}Pb/^{204}Pb$ | $^{208}Pb/^{204}Pb$ | $^{207}Pb/^{206}Pb$ | $^{208}Pb/^{207}Pb$ | $^{206}Pb/^{207}Pb$ | μ |
|---|---|---|---|---|---|---|---|---|---|
| 1 | 07-1-5 | 闪锌矿 | 18.390 | 15.733 | 38.492 | 0.8555 | 2.447 | 1.1689 | 9.73 |
| 2 | GQO-24-2 | 闪锌矿 | 18.477 | 15.848 | 38.734 | 0.8577 | 2.444 | 1.1659 | 9.95 |
| 3 | GQO-24-3 | 闪锌矿 | 18.476 | 15.869 | 38.711 | 0.8589 | 2.439 | 1.1643 | 9.99 |
| 4 | 6#kengB1 | 闪锌矿 | 18.158 | 15.633 | 38.096 | 0.8610 | 2.437 | 1.1615 | 9.56 |
| 5 | 6#kengB3 | 闪锌矿 | 18.362 | 15.758 | 38.467 | 0.8582 | 2.441 | 1.1652 | 9.78 |
| 6 | MY6-QGr2 | 闪锌矿 | 18.513 | 15.895 | 38.786 | 0.8586 | 2.440 | 1.1647 | 10.04 |
| 7 | MY6-QGH4 | 闪锌矿 | 18.201 | 15.668 | 38.163 | 0.8608 | 2.436 | 1.1617 | 9.62 |
| 8 | MY6-QGH8 | 闪锌矿 | 18.179 | 15.658 | 38.153 | 0.8614 | 2.437 | 1.161 | 9.61 |
| 9 | MY6-QGH14 | 闪锌矿 | 18.344 | 15.791 | 38.499 | 0.8608 | 2.438 | 1.1616 | 9.85 |
| 10 | 6#kengB1 | 方铅矿 | 18.210 | 15.705 | 38.252 | 0.8625 | 2.436 | 1.1595 | 9.7 |
| 11 | 6#kengB3 | 方铅矿 | 18.248 | 15.675 | 38.276 | 0.8590 | 2.442 | 1.1641 | 9.63 |
| 12 | MY6-QGH4 | 方铅矿 | 18.197 | 15.683 | 38.192 | 0.8618 | 2.435 | 1.1603 | 9.65 |
| 13 | MY6-QGH8 | 方铅矿 | 18.186 | 15.685 | 38.243 | 0.8625 | 2.438 | 1.1594 | 9.66 |
| 14 | MY6-QGH14 | 方铅矿 | 18.230 | 15.699 | 38.262 | 0.8611 | 2.437 | 1.1613 | 9.68 |
| 15 | 6#kengB3 | 黄铁矿 | 18.237 | 15.654 | 38.163 | 0.8583 | 2.438 | 1.165 | 9.59 |
| 16 | MY6-QGr2 | 黄铁矿 | 18.251 | 15.672 | 38.226 | 0.8587 | 2.439 | 1.1645 | 9.62 |

| 序号 | 样品编号 | 样品名称 | ω | Th/U | V1 | V2 | △α | △β | △γ |
|---|---|---|---|---|---|---|---|---|---|
| 1 | 07-1-5 | 闪锌矿 | 38.1 | 3.79 | 75.9 | 64.7 | 86.23 | 27.56 | 42.22 |
| 2 | GQO-24-2 | 闪锌矿 | 39.74 | 3.87 | 89.61 | 72.77 | 97.36 | 35.49 | 52.03 |
| 3 | GQO-24-3 | 闪锌矿 | 39.84 | 3.86 | 90.9 | 74.74 | 99.33 | 36.98 | 52.5 |
| 4 | 6#kengB1 | 闪锌矿 | 36.79 | 3.72 | 63.79 | 57.75 | 76.33 | 21.27 | 33.59 |
| 5 | 6#kengB3 | 闪锌矿 | 38.4 | 3.8 | 78.32 | 66.74 | 88.62 | 29.47 | 43.75 |
| 6 | MY6-QGr2 | 闪锌矿 | 40.2 | 3.88 | 93.99 | 76.56 | 101.86 | 38.71 | 54.71 |
| 7 | MY6-QGH4 | 闪锌矿 | 37.16 | 3.74 | 67.32 | 60.51 | 79.74 | 23.62 | 35.85 |
| 8 | MY6-QGH8 | 闪锌矿 | 37.15 | 3.74 | 66.86 | 59.53 | 78.81 | 23.01 | 35.8 |
| 9 | MY6-QGH14 | 闪锌矿 | 38.95 | 3.83 | 82.48 | 68.92 | 91.73 | 31.92 | 46.86 |
| 10 | 6#kengB1 | 方铅矿 | 37.84 | 3.78 | 72.56 | 62.77 | 83.34 | 26.28 | 39.92 |
| 11 | 6#kengB3 | 方铅矿 | 37.44 | 3.76 | 69.37 | 60.4 | 80.44 | 23.94 | 37.79 |
| 12 | MY6-QGH4 | 方铅矿 | 37.45 | 3.76 | 69.45 | 61.38 | 81.17 | 24.7 | 37.53 |
| 13 | MY6-QGH8 | 方铅矿 | 37.76 | 3.78 | 71.25 | 60.88 | 81.4 | 24.92 | 39.42 |
| 14 | MY6-QGH14 | 方铅矿 | 37.71 | 3.77 | 71.65 | 62.33 | 82.7 | 25.7 | 39.22 |
| 15 | 6#kengB3 | 黄铁矿 | 36.83 | 3.72 | 65.06 | 59.77 | 78.43 | 22.47 | 33.98 |
| 16 | MY6-QGr2 | 黄铁矿 | 37.19 | 3.74 | 67.85 | 60.79 | 80.21 | 23.73 | 36.21 |

注：$\mu=^{238}U/^{204}Pb$，表征$^{238}U$的富集程度；$\omega=^{232}Th/^{204}Pb$，表征$^{232}Th$的富集程度；特征值$Th/U=0.96776\times\omega/\mu$；V1、V2、△α、△β、△γ为矢量参数(朱炳泉, 1998)。

**表3 松梁Pb-Zn矿床闪锌矿锌同位素组成**

**Table 3 Zinc isotopic compositions of sphalerite from the Songliang Pb-Zn deposit**

| 序号 | 样品编号 | 样品名称 | $\delta^{66}Zn_{IRMM-3702}$/‰ | 2σ/‰ | $\delta^{68}Zn_{IRMM-3702}$/‰ | 2σ/‰ |
|---|---|---|---|---|---|---|
| 1 | 07-1-5 | 闪锌矿 | −0.126 | 0.057 | −0.237 | 0.066 |
| 2 | GQO-24-2 | 闪锌矿 | 0.078 | 0.051 | 0.141 | 0.064 |
| 3 | GQO-24-3 | 闪锌矿 | 0.082 | 0.063 | 0.155 | 0.074 |
| 4 | MY6-QGH4 | 闪锌矿 | 0.032 | 0.062 | 0.054 | 0.069 |
| 5 | MY6-QGH14 | 闪锌矿 | −0.023 | 0.060 | −0.030 | 0.069 |
| 6 | 6#KengB1 | 闪锌矿 | −0.003 | 0.062 | 0.009 | 0.064 |

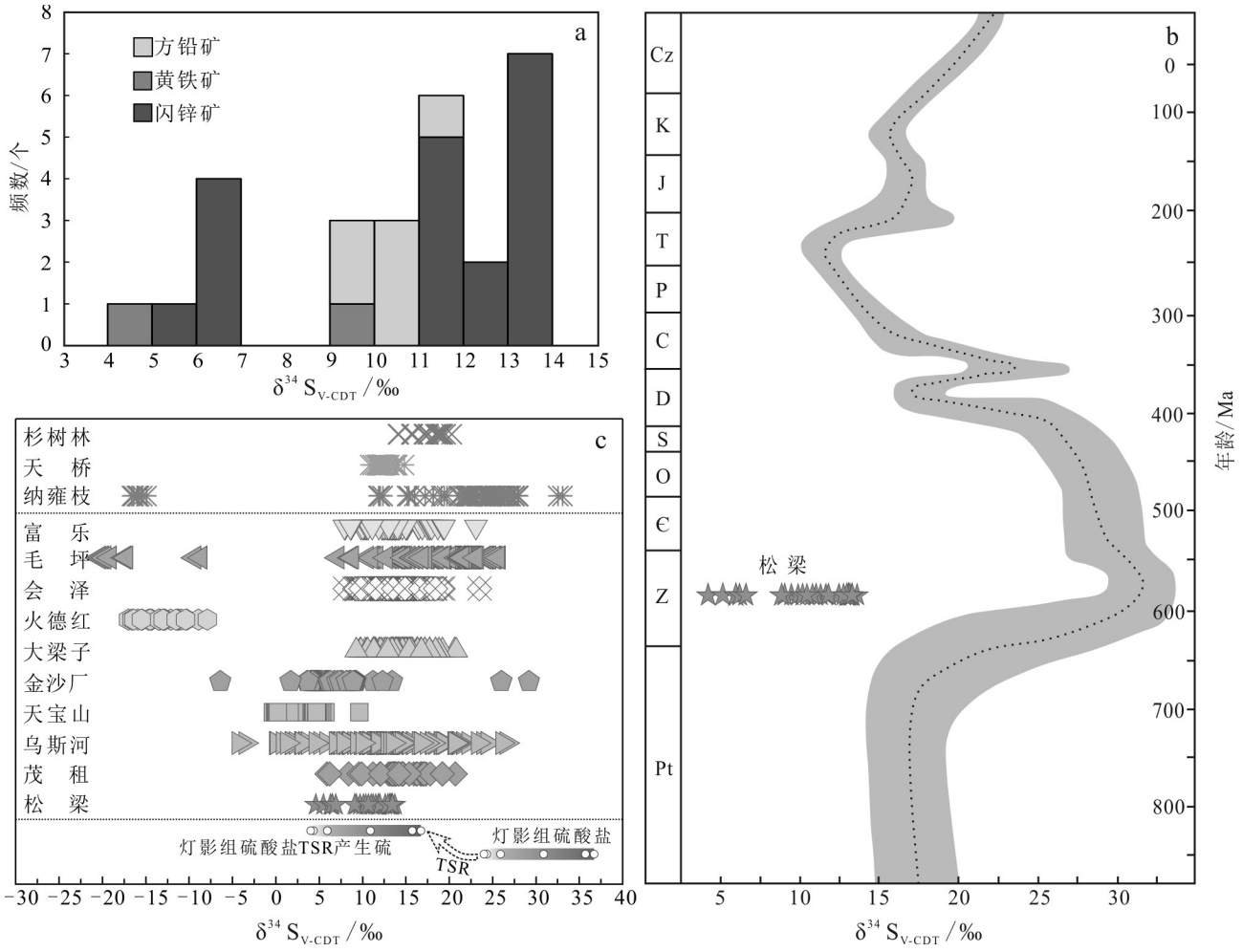


图 5　松梁 Pb-Zn 矿床硫化物的硫同位素直方图(a)、硫同位素组成与海相硫酸盐 (b,底图据 Claypool et al., 1980 修改)及其与其他 Pb-Zn 矿床的对比(c)

数据来源:杉树林(Zhou et al., 2014a);天桥(Zhou et al., 2014b);纳雍枝(金中国等, 2016; 杨兴玉等, 2018; Zhou et al., 2018b; Wei et al., 2021b);富乐(付绍洪, 2004; Zhou et al., 2018a; 任涛等, 2019);毛坪(任顺利等, 2018; 谈树成等, 2019; He et al., 2020; Xiang et al., 2020; 杨清, 2021);会泽(付绍洪, 2004; 李文博等, 2004; 韩润生等, 2006; 吴越, 2013; 王磊等, 2016);火德红(金灿海等, 2016; 武昱东等, 2016);大梁子(付绍洪, 2004; 吴越, 2013; 袁波等, 2014; 刘志鹏, 2016; 王海等, 2018; Zhu et al., 2020);金沙厂(Bai et al., 2013);天宝山(付绍洪, 2004; Zhou et al., 2013b; 何承真等, 2016; Zhu et al., 2016; Tan et al., 2019);乌斯河(Zhu et al., 2018; Zhang et al., 2019a; Luo et al., 2020; Wei et al., 2020);茂租(Zhou et al., 2013a; Wang et al., 2018; Zhang et al., 2019b);灯影组硫酸盐(Goldberg et al., 2005)

Fig. 5　Histogram of S isotope compositions of sulfides from the Songliang Pb-Zn deposit (a) and comparison of the S isotopic compositions of the sulfides from the Songliang with marine sulfate (b, base map modified after Claypool et al., 1980) and other Pb-Zn deposits in SYG (c)

Data source: Shanshulin (Zhou et al., 2014a), Tianqiao (Zhou et al., 2014b), Nayongzhi (Jin et al., 2016; Yang et al., 2018; Zhou et al., 2018b; Wei et al., 2021b), Fule ( Fu, 2004; Zhou et al., 2018a; Ren et al., 2019), Maoping (Ren et al., 2018; Tan et al., 2019; He et al., 2020; Xiang et al., 2020; Yang, 2021), Huize (Fu, 2004; Li et al., 2004; Han et al., 2006; Wu, 2013; Wang et al., 2016), Huodehong (Jin et al., 2016; Wu et al., 2016), Dangliangzi (Fu, 2004; Wu, 2013; Yuan et al., 2014; Liu, 2016; Wang et al.,2018; Zhu et al., 2020), Jinshachang (Bai et al., 2013), Tianbaoshan (Fu, 2004; Zhou et al., 2013b; He et al., 2016; Zhu et al., 2016; Tan et al., 2019), Wusihe (Zhu et al., 2018; Zhang et al., 2019a; Luo et al., 2020; Wei et al., 2020), Maozu (Zhou et al., 2013a; Wang et al., 2018; Zhang et al., 2019b), Dengying Formation sulphate (Goldberg et al., 2005)

大梁子等铅锌矿床一致(图 5c; Wang et al., 2018; Zhang et al., 2019 b; Zhu et al., 2020)。

川滇黔地区大部分铅锌矿床的还原硫主要来自沉积物,Zhu 等 (2020)按照 $\delta^{34}S$ 值变化区间将该区域铅锌矿床分为 2 大类:① 诸如富乐、茂租、大梁子、会泽等矿床,$\delta^{34}S$ 值范围在 11‰~19‰,明显大

于幔源硫(0±3‰),与同时期海水硫酸盐的$\delta^{34}S$值相近,还原硫由硫酸盐热化学还原作用(TSR)形成;② 如天宝山、金沙厂矿床,$\delta^{34}S$值范围在4‰~7‰,略大于幔源硫,但远低于同时期海水硫酸盐。本文将川滇黔区域内部分铅锌矿床的S-Pb同位素绘制二元图解(图6),可圈出3个区域;$\delta^{34}S$值变化范围与上述Zhu等(2020)提出的两大分类基本一致,并在此基础上可增添第三类:③如还原硫可能由硫酸盐生物成因还原作用(BSR)形成的火德红矿床,其$\delta^{34}S$值为负值,$\Delta^{34}S_{SO_4\text{-}H_2S}$大于30‰(火德红$\delta^{34}S$值:−10.4‰ −16.4‰,赋矿地层中泥盆统的同时期海相硫酸盐$\delta^{34}S$值:+17.5‰~+26.5‰;金灿海等, 2016;武昱东等, 2016)。图6显示松梁矿床大部分$\delta^{34}S$值位于①类范围内,但有少数几个数据点落于②类范围。针对天宝山和金沙厂此类矿床,其硫来源存在争议,Zhu 等(2016)认为,天宝山矿床还原硫是在TSR作用下由赋矿地层经蒸发淋滤形成;何承真等(2016)认为,天宝山铅锌矿床成矿流体中的硫来源于地幔和上震旦统灯影组白云岩源区的混合作用。金沙厂矿床因其矿物组成有重晶石($BaSO_4$)与硫化物共存,其硫化物还原硫可能与岩浆活动有关,受壳源硫和TSR产生还原硫的影响(Bai et al., 2013)。综合来看,松梁铅锌矿床落入②类范围内的个别数据点可能是由TSR过程中成矿温度变化所致(Xu et al., 2020)。

### 5.2 铅同位素

硫化物的Th和U含量非常低,因而放射性成因Pb可忽略不计,铅同位素组成接近矿化流体的初始铅同位素组成(Pass et al., 2014)。$^{207}Pb/^{204}Pb$-$^{206}Pb/^{204}Pb$图解(图7a)中,松梁铅锌矿床数据点大部分投影在上地壳铅演化曲线附近,少数位于造山带和上地壳造山带铅生长演化曲线之间。铅同位素组成△β-△γ图(图7c)中,松梁铅锌矿床与川滇黔地区部分铅锌矿类似,大部分数据点位于上地壳铅区域,部分数据点位于上地壳与地幔混合的俯冲带铅区域内,表明松梁铅锌矿床的Pb源自上地壳。

松梁矿床的铅同位素数据变化范围较窄,表明成矿金属的来源较为单一或混合多个铅同位素组成相似的源区。$^{208}Pb/^{204}Pb$-$^{206}Pb/^{204}Pb$图解(图7b)中,松梁矿床的铅同位素数据分布呈明显的线性相关趋势,反映出该矿床硫化物Pb可能来自单个均匀的同位素储层或具不同铅同位素组成特征的2个储层的混合(Zartman et al., 1981)。已有的研究表明,川滇黔成矿域的潜在成矿物质来源主要为元古代基底岩、震旦纪—中二叠世沉积岩及晚二叠世峨眉山玄武岩(金中国等,2016; Wang et al., 2018),这3种源区金属物质的提供模式和比例决定了不同铅锌矿床的铅同位素组成。将区域结晶基底(昆阳群、会理群)、峨眉山玄武岩、震旦系灯影组白云岩和各时代碳酸盐岩的沉积地层铅同位素组成投影到$^{207}Pb/^{204}Pb$-$^{206}Pb/^{204}Pb$图(图7a)中,松梁铅锌矿床的铅同位素主要集中于震旦系灯影组白云岩和结晶基底的铅同位素范围内,极少数样品落入峨眉山玄武岩或泥盆系至二叠系碳酸盐岩盖层区域内。与川滇黔成矿域内典型铅锌矿床铅同位素对比,松梁矿床的铅同位素组成与赋存于震旦系灯影组的大梁子、茂租等铅锌矿床高度一致,指示它们可能具有相似的铅源;而显著不同于赋存于其他时代地层的会泽、毛坪、富乐和纳雍枝等矿床。因此,松梁矿床的成矿物质壳源铅由震旦系灯影组白云岩和川滇黔区域结晶基底提供。

### 5.3 锌同位素

锌同位素可用于示踪热液系统中锌的提取、搬运和沉淀的地球化学过程(Pašava et al., 2014; Duan et al., 2016)。前人对不同类型矿床(VMS型、MVT型矿床)和现代海底热液系统的研究表明,闪锌矿的锌同位素组成受控于源岩以及沉淀过程中与温度有关的动力学分馏(Mason et al., 2005; Wilkinson et al., 2005; John et al., 2008; Kelley et al., 2009)。$^{64}Zn$富集的硫化物主要出现在热液系统的早期,而残余流体和后期沉积物的$\delta^{66}Zn$值较高;热液与闪锌矿的锌同位素分馏值一般在0~+0.2‰之间(Archer et al., 2004; Fujii et al., 2011; Gagnevin et al., 2012)。

热液系统中的锌同位素分馏主要经历矿物学分馏、淋滤作用、沉淀作用3种过程(Mason et al., 2005)。其中,沉淀作用过程中又受控于4种因素:① 动力瑞利分馏、② 温度变化、③ 源岩或不同来源锌的混合、④ 生物(有机质)(Wilkinson et al., 2005; John et al., 2008; Kelley et al., 2009)。前人研究表明,无论是在实验中(30~50°C,Maréchal et al., 2002)或是在热液系统中(60~250° C, Wilkinson et al., 2005),中低温度(< 300°C)条件下的$\delta^{66}Zn$值与温度之间不存在相关性。松梁铅锌矿床所处的川滇黔成矿域,同样也是著名的华南低温成矿域(胡瑞忠等,2020),因此可以确定松梁铅锌矿床$\delta^{66}Zn$值与温度无关。

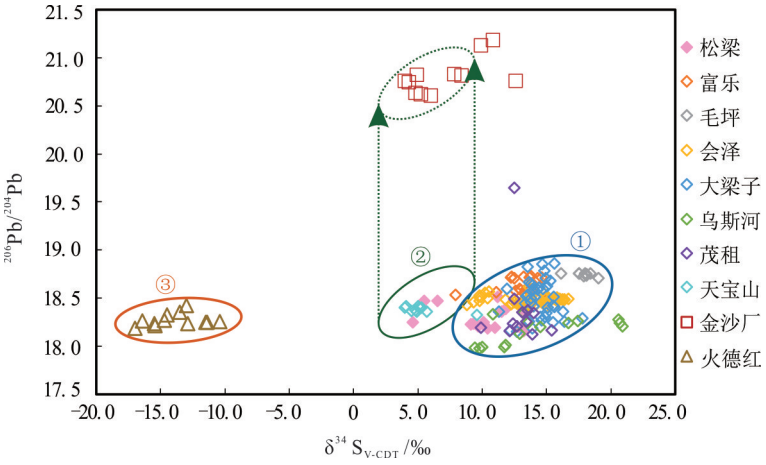


图 6　川滇黔成矿域部分 Pb-Zn 矿床 $\delta^{34}S_{V\text{-}CDT}$-$^{206}Pb/^{204}Pb$ 图解

①②③代表川滇黔成矿域部分铅锌矿床根据 $\delta^{34}S$ 区间划分的类别序号

数据来源:富乐(付绍洪, 2004; 任涛等, 2019);毛坪(He et al., 2020);会泽(付绍洪, 2004; 李文博等, 2006);大梁子(付绍洪, 2004; 刘志鹏, 2016; Zhu et al., 2020);乌斯河(Zhu et al., 2018);茂租(Zhou et al., 2013b);天宝山(付绍洪, 2004; Zhou et al., 2013b);金沙厂(Xu et al., 2020);火德红(金灿海等, 2016; 武昱东等, 2016)

Fig. 6　$\delta^{34}S_{V\text{-}CDT}$-$^{206}Pb/^{204}Pb$ diagram of some Pb-Zn deposits in the Sichuan-Yunnan-Guizhou metallogenic province

①②③ represent the classification numbers of some Pb-Zn deposits in the SYG metallogenic Province according to the $\delta^{34}S$ interval

Data source: Fule (Fu, 2004; Ren et al., 2019), Maoping (He et al., 2020), Huize (Fu, 2004; Li et al., 2006), Daliangzi (Fu, 2004; Liu, 2016; Zhu et al., 2020), Wusihe (Zhu et al., 2018), Maozu (Zhou et al., 2013b), Tianbaoshan (Fu, 2004; Zhou et al., 2013b), Jinshachang (Xu et al., 2020), Huodehong (Jin et al., 2016; Wu et al., 2016)

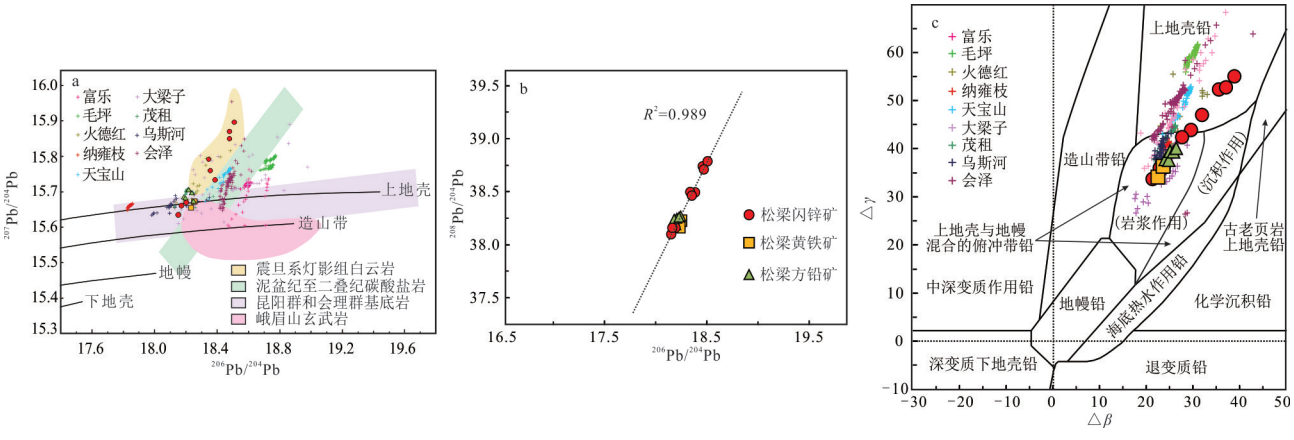


图 7　松梁 Pb-Zn 矿床与川滇黔地区部分铅锌矿床铅同位素组成与晚二叠世峨眉山玄武岩、埃迪卡拉—中二叠世沉积岩、元古代变质岩的 Pb 同位素组成对比(a,底图据 Zartman et al., 1981;朱炳泉等,1998)、松梁矿床硫化物 $^{208}Pb/^{204}Pb$-$^{206}Pb/^{204}Pb$ 图(b)及松梁铅锌矿床铅同位素组成 $\Delta\beta$-$\Delta\gamma$ 图(c,底图据朱炳泉等,1998)

数据来源:富乐(付绍洪, 2004; Zhou et al., 2018a; 任涛等, 2019);毛坪(谈树成等, 2019; He et al., 2020; Xiang et al.,2020; Wu et al.,2021);火德红(金灿海等,2016; 武昱东等, 2016);纳雍枝(金中国等, 2016);天宝山(付绍洪, 2004; Zhou et al., 2013b; Tan et al., 2019);大梁子(付绍洪, 2004; 刘志鹏, 2016; 王海等, 2018; Zhu et al., 2020);茂租(Zhou et al., 2013a; Wang et al., 2018);乌斯河(Zhu et al., 2018; Wei Chen et al.,2020);会泽(付绍洪, 2004; 李文博等, 2006)

Fig. 7　Comparison of Pb isotope compositions between the Songliang deposit and some Pb-Zn deposits in SYG and the Pb isotope compositions of the Late Permian Emeishan basalts, Late Ediacaran-Middle Permian sedimentary rocks, and Proterozoic metamorphic rocks(a, base map after Zartman et al., 1981; Zhu et al., 1998 ), plots of $^{208}Pb/^{204}Pb$-$^{206}Pb/^{204}Pb$(b) and $\Delta\beta$-$\Delta\gamma$ diagram of Pb isotope composition of the Songliang Pb-Zn deposit (c, base map after Zhu et al., 1998)

Data source: Fule (Fu, 2004; Zhou et al., 2018a; Ren et al., 2019), Maoping (Tan et al., 2019; He et al., 2020; Xiang et al., 2020; Wu et al., 2021), Huodehong (Jin et al., 2016; Wu et al., 2016), Nayongzhi (Jin et al., 2016), Tianbaoshan (Fu, 2004; Zhou et al., 2013b; Tan et al., 2019), Daliangzi (Fu, 2004; Liu, 2016; Wang et al., 2018; Zhu et al., 2020), Maozu (Zhou et al., 2013a; Wang et al., 2018), Wusihe (Zhu et al., 2018; Wei Chen et al., 2020), Huize (Fu, 2004; Li et al., 2006)

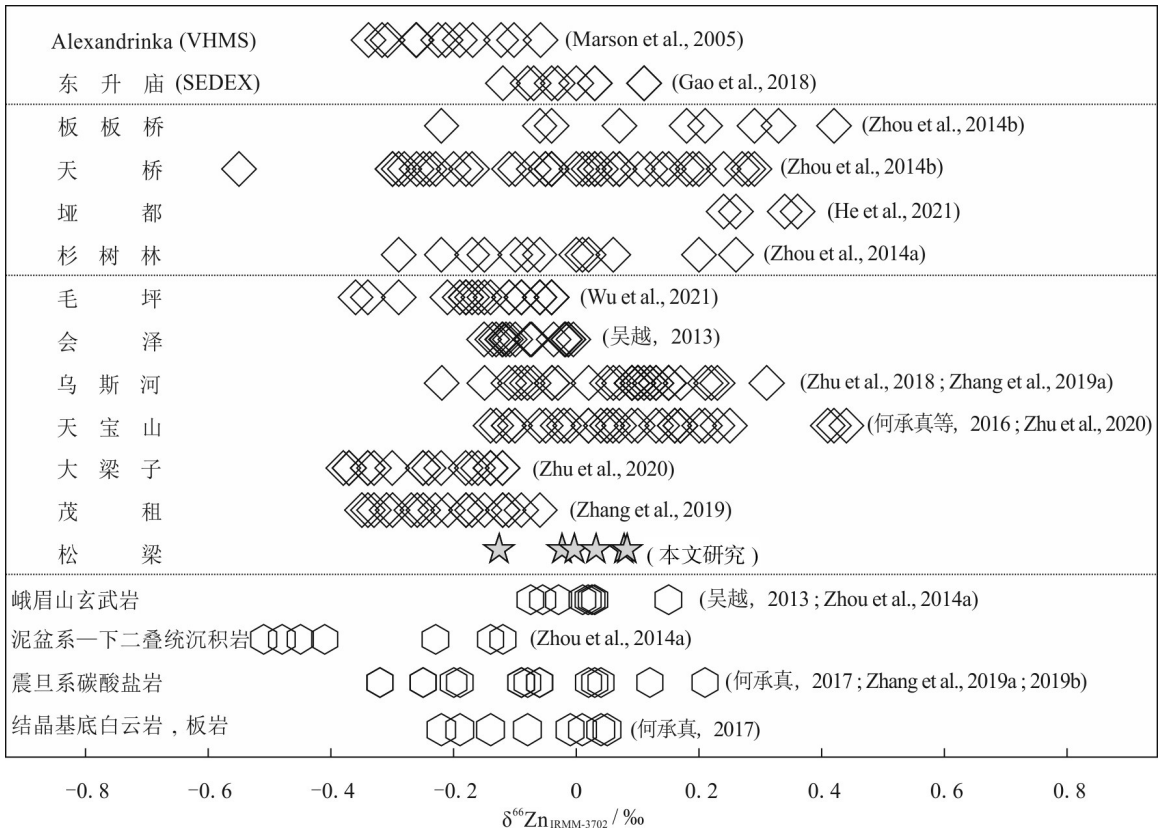


图 8 川滇黔地区部分 Pb-Zn 矿床与典型 VHMS 和 SEDEX 型铅锌矿床闪锌矿的锌同位素组成

Fig. 8 Zn isotope variation of sphalerite from Pb-Zn deposits in SYG and typical VHMS and SEDEX Pb-Zn deposits

松梁矿床闪锌矿的 $\delta^{66}Zn_{IRMM-3702}$ 值介于−0.126‰~+0.082‰，处于震旦系碳酸盐岩锌同位素组成(−0.32‰~+0.21‰)范围内，基本与结晶基底锌同位素组成(−0.22‰~+0.05‰)一致，大于泥盆系—下二叠统沉积岩的锌同位素组成(−0.51‰~−0.12‰)，其阈值略小于峨眉山玄武岩锌同位素组成(−0.075‰~+0.15‰；图 7)；表明松梁矿床存在 2 个 Zn 源：震旦系碳酸盐岩和结晶基底。值得注意的是，川滇黔区域铅锌成矿时代与峨眉山玄武岩浆活动时限相差久远，峨眉山玄武岩浆活动与铅锌成矿只是空间上的重合、并没有直接的成因联系，但不排除成矿流体活化峨眉山玄武岩中的部分成矿元素(黄智龙等, 2001; 李波等, 2012; 周家喜等, 2012)。因此，松梁矿床的锌源自震旦系碳酸盐岩和结晶基底的混合，峨眉山玄武岩为潜在锌源。

会泽铅锌矿床闪锌矿锌同位素组成集中，$\delta^{66}Zn_{IRMM-3702}$ 值介于 − 0.151‰~ + 0.005‰，均值为 −0.081‰(图 8)，按其从流体中晶出先后顺序，未表现出规律性变化，与松梁铅锌矿床的锌同位素组成相似。吴越(2013)认为会泽矿床成矿流体的锌同位素组成均一，闪锌矿晶出前成矿流体经过充分“均一化”过程(黄智龙等, 2004)。何承真等(2016)报道了天宝山矿床锌同位素组成，其微区样品 $\delta^{66}Zn_{IRMM-3702}$ 值介于+0.1‰~+0.23‰，均值+0.169‰，结合 S 同位素数据，表明同一手标本的闪锌矿微区样品具有均一的锌同位素组成；3 个中段闪锌矿锌同位素组成范围变化较大，$\delta^{66}Zn_{IRMM-3702}$ 值介于−0.14‰~+0.44‰，均值为−0.092‰，该变化主要受成矿流体中锌同位素和成矿流体的迁移就位途径控制。

### 5.4 成矿物质来源

松梁矿床的铅锌矿体主要赋存于震旦系灯影组白云岩中，主要呈脉状、透镜体状，严格受断裂控制，后生成矿特征明显；其矿物组成简单，围岩蚀变单一，主要有白云石化、方解石化、硅化、重晶石化、黄铁矿化等，反映出中、低温热液成矿的特征，同川滇黔成矿域内多数矿床一样，与典型的 MVT 矿床具有相似之处，可能是大规模流体活动的结果(黄智龙等, 2004)，但对于该域铅锌矿床成矿物质来源

与演化过程,以及矿床成因仍存在较大争议。

本文同位素地球化学研究表明,松梁铅锌矿床的成矿物质硫源自震旦系灯影组地层,成矿物质铅源自震旦系灯影组白云岩和结晶基底的混合,成矿物质锌源自震旦系碳酸盐岩和结晶基底的混合,峨眉山玄武岩为潜在锌源。考虑到该域内铅锌矿床相较典型MVT矿床的特殊性,本文暂将松梁铅锌矿床定为后生碳酸盐岩容矿型铅锌矿床。

## 6 结　论

(1) 松梁铅锌矿床的硫化物$\delta^{34}S_{CDT}$值在+4.6‰~+13.7‰之间,平均值为+10.5‰;硫来源于赋矿围岩,为震旦系灯影组蒸发岩经TSR反应的产物。

(2) 铅同位素组成反映成矿物质为壳源铅,源自震旦系灯影组白云岩与结晶基底的混合。

(3) 锌同位素组成表明成矿物质源自震旦系灯影组碳酸盐岩和结晶基底的混合,峨眉山玄武岩为潜在锌源;松梁铅锌矿床为后生碳酸盐岩容矿型铅锌矿床。

**References**


Archer C, Vance D and Butler I. 2004. Abiotic Zn isotope fractionations associated with ZnS precipitation[J]. Geochimica et Cosmochimica Acta, 68: A325.

Bai J H, Huang Z L, Zhu Dan, Yan Z F and Zhou J X. 2013. Isotopic compositions of sulfur in the Jinshachang lead-zinc deposit, Yunnan, China, and its implication on the formation of sulfur-bearing minerals[J]. Acta Geologica Sinica(English Edition), 87(5): 1355-1369.

Claypool G E, Holser W T, Kaplan I R, Sakai H and Zak I. 1980. The age curves of sulfur and oxygen isotopes in marine sulfate and their mutual interpretation[J]. Chemical Geology, 28: 199-260.

Duan J, Tang J and Lin B. 2016. Zinc and lead isotope signatures of the Zhaxikang Pb-Zn deposit, South Tibet: Implications for the source of the ore-forming metals[J]. Ore Geology Reviews, 78: 58-68.

Fu J N, Pirajno F, Yang F, Shivute E, Sun Y Z, Ai N and Qiu K F. 2021. Integration of zircon and apatite U-Pb geochronology and geochemical mapping of the Wude basalts(Emeishan large igneous province): A tool for a better understanding of the tectonothermal and geodynamic evolution of the Emeishan LIP[J]. Geoscience Frontiers, 12(2): 573-585.

Fu S H. 2004. Metallogenesis of Pb-Zn deposits and enrichment regularity of dispersed elements Cd, Ga and Ge in SW Yangtze block (dissertation for Master degree)[D]. Supervisor: Gu X X. Chengdu: Chengdu University of Technology. 94p(in Chinese with English abstract).

Fujii T, Moynier F, Pons M L and Albarède F. 2011. The origin of Zn isotope fractionation in sulfides[J]. Geochimica et Cosmochimica Acta, 75(23): 7632-7643.

Gagnevin D, Boyce A J, Barrie C D, Menuge J F and Blakeman R J. 2012. Zn, Fe and S isotope fractionation in a large hydrothermal system[J]. Geochimica et Cosmochimica Acta, 88: 183-198.

Goldberg T, Poulton S W and Strauss H. 2005. Sulphur and oxygen isotope signatures of late Neoproterozoic to Early Cambrian sulphate, Yangtze Platform, China: Diagenetic constraints and seawater evolution[J]. Precambrian Research, 137(3): 223-241.

Han R S, Chen J, Huang Z L, Ma D Y, Xue C D, Li Y, Zou H J, Li B, Hu Y Z, Ma G S, Huang D Y and Wang X K. 2006. Dynamics of tectonic ore-forming processes and localization-prognosis of concealed orebodies-As exemplified by the Huize super-large Zn-Pb-(Ag-Ge) district, Yunnan[M]. Beijing: Science Press. 239p(in Chinese).

Han R S, Hu Y Z, Wang X K, Hou B H, Huang Z L, Chen J, Wang F, Wu P, Li B, Wang H J, Dong Y and Lei L. 2012. Mineralization model of rich Ge-Ag-bearing Zn-Pb polymetalic deposit concentrated district in northeastern Yunnan, China[J]. Acta Geologica Sinica, 86(2): 280-294(in Chinese with English abstract).

He C S, Santosh M, Wu J P and Chen X H. 2014. Plume or no plume: Emeishan Large Igneous Province in Southwest China revisited from receiver function analysis[J]. Physics of the Earth and Planetary Interiors, 232: 72-78.

He C Z, Xiao C Y, Wen H J, Zhou T, Zhu C W and Fan H F. 2016. Zn-S isotope composition of the Tianbaoshan carbonate-hosted Pb-Zn deposit in Sichuan, China: Implication for source of ore components[J]. Acta Petrologica Sinica, 32(11): 3394-3406(in Chinese with English abstract).

He C Z. 2017. Zinc and Sulfur isotopic compositions of the Tianbaoshan carbonate-hosted Pb-Zn deposit in Sichuan, China: Implications for source of ore components (dissertation for Master degree)[D]. Supervisor: Fan H F; Lu D B. Guiyang: Institute of Geochemistry, Chinese Academy of Sciences. 65p(in Chinese with English abstract).

He Y F, Wu T, Huang Z L, Ye L and Deng P. 2020. Genesis of the Maoping carbonate-hosted Pb-Zn deposit, northeastern Yunnan Province, China: Evidences from geology and C-O-S-Pb isotopes[J]. Acta Geochimica, 39(5): 782-796.

He Z W, Li Z Q, Li B, Chen J, Xiang Z P, Wang X F, Du L J and Huang Z L. 2021. Ore genesis of the Yadu carbonate-hosted Pb-Zn deposit in Southwest China: Evidence from rare earth elements and C, O, S, Pb and Zn isotopes[J]. Ore Geology Reviews, 131:104039.

Hoefs J. 2018. Stable isotope geochemistry[M]. Berlin: Springer-Verlag. 389p.

Hu R Z, Chen W, Bi X W, Fu S L, Yin R S and Xiao J F. 2020. Control

of the Precambrian basement on the formation of the Mesozoic large-scale low-temperature mineralization in the Yangtze Craton[J]. Earth Science Frontiers, 27(2): 137-150(in Chinese with English abstract).

Hu R Z, Fu S L, Huang Y, Zhou M F, Fu S H, Zhao C H, Wang Y J, Bi X W and Xiao J F. 2017. The giant South China Mesozoic low-temperature metallogenic domain: Reviews and a new geodynamic model[J]. Journal of Asian Earth Sciences, 137: 9-34.

Huang Y, He C, Chen N S and Xia B. 2019. Diabase sills in the outer zone of the Emeishan Large Igneous Province, Southwest China: Petrogenesis and tectonic implications[J]. Journal of Earth Science, 30(4):739-753.

Huang Z L, Chen J, Liu C Q, Han R S, Li W B, Zhao D S, Gao D R and Feng Z H. 2001. A preliminary discussion on the genetic relationship between emeishan basalts and Pb-Zn deposits as exemplified by the Huize Pb-Zn deposit, Yunnan Province[J]. Acta Mineralogica Sinica, 21(4): 681-688(in Chinese with English abstract).

Huang Z L, Li W B, Zhang Z L, Han R S and Chen J. 2004. Several problems involved in genetic studies on Huize superlarge Pb-Zn deposit, Yunnan Province[J]. Acta Mineralogica Sinica, 24(2): 105-111(in Chinese with English abstract).

Jin C H, Zhang Y, Shen Z W and Zhang D. 2016. Geological characteristics and metallogenic material source of the Huodehong Pb-Zn deposit, Northeast Yunnan Province[J]. Mineralogy and Petrology, 36(4): 50-56(in Chinese with English abstract).

Jin Z G, Zhou J X, Huang Z L, Luo K, Gao J G, Peng S, Wang B and Chen X L. 2016. Ore genesis of the Nayongzhi Pb-Zn deposit, Puding City, Guizhou Province, China: Evidences from S and in situ Pb isotopes[J]. Acta Petrologica Sinica, 32(11): 3441-3455(in Chinese with English abstract).

John S G, Rouxel O J, Craddock P R, Engwall A M and Boyle E A. 2008. Zinc stable isotopes in seafloor hydrothermal vent fluids and chimneys[J]. Earth and Planetary Science Letters, 269(1): 17-28.

Kelley K D, Wilkinson J J, Chapman J B, Crowther H L and Weiss D J. 2009. Zinc isotopes in sphalerite from base metal deposits in the Red Dog district, Northern Alaska[J]. Econ. Geol., 104(6): 767-773.

Kong Z G, Wu Y, Zhang F, Zhang C Q, Meng X Y. 2018. Sources of ore-forming material of typical Pb-Zn deposits in the Sichuan-Yunnan-Guizhou Metalogenic Province: Constraints from the S-Pb isotopic compositions[J]. Earth Science Frontiers, 25(1): 125-137(in Chinese with English abstract).

Lefticariu L, Behum P T, Bender K S and Lefticariu M. 2017. Sulfur isotope fractionation as an indicator of biogeochemical processes in an AMD passive bioremediation system[J]. Minerals, 7(41): 1-20.

Li B. 2008. Geological characteristics and tectonic geochemistry anomaly model of Qiaojia Songliang lead and zinc deposit in the Yunnan Province, Southwest of China (dissertation for Master degree)[D]. Supervisor: Han R S and Gu X C. Kunming: Kunming University of Science and Technology. 116p(in Chinese with English abstract).

Li B. 2010. The study of fluid inclusions geochemistry and tectonic geochemistry of lead-zinc deposits: Taking Huize and Songliang lead-zinc deposits for examples, in the northeast of Yunnan Province, China (dissertation for doctor degree)[D]. Supervisor: Han R S and Gu X C. Kunming: Kunming University of Science and Technology. 194p(in Chinese with English abstract).

Li B, Gu X C, Han R S, Wen S M, Xu G R, Cao Y, Wu H, Zou G F, Sheng R. 2012. Geological characteristics and metalogenic geological conditions of the Songliang lead-zinc deposit, Northeast of Yunnan[J]. Mineral Resources and Geology, 26(1): 13-18+67 (in Chinese with English abstract).

Li B, Han R S, Wen S M, Sheng R, Qiu W L and Tang G. 2014. Structural characteristics and fault tectono-geochemistry of the Songliang lead-zinc deposit in Northeast Yunnan, China[J]. Geotectonica et Metallogenia, 38(4):855-865(in Chinese with English abstract).

Li W B, Huang Z L, Chen J, Xv C, Guan T and Yin M D. 2004. Sulfur isotopes and rare-earth elements geochemistry of the giant Huize Zn-Pb deposit in Yunnan Province[J]. Acta Geologica Sinica, (4): 507-518(in Chinese with English abstract).

Li W B, Huang Z L and Zhang G. 2006. Sources of ore metals of the Huize ore field in Yunnan Province: Constraints from Pb, S, C, H, O and Sr isotope geochemistry[J]. Acta Petrologica Sinica, 22 (10): 2567-2580 (in Chinese with English abstract).

Li Y H. 2020. Guest Editor's Preface to the "New technologies of isotope analysis and its applications in geology"[J]. Acta Geoscientica Sinica, 41(5): 583-589(in Chinese with English abstract).

Li Z L, Ye L, Hu Y S and Huang Z L. 2018. Geological significance of nickeliferous minerals in the Fule Pb-Zn deposit, Yunnan Province, China[J]. Acta Geochimica, 37(5): 684-690.

Liao W. 1984. Characteristics of S, Pb isotopic composition and discussion on genesis of the Pb-Zn metallic deposit in eastern and western Yunnan[J]. Geology and Prospecting, (1): 2-6(in Chinese with English abstract).

Liu Z P. 2016. General study on the stable isotope geochemistry of the Daliangzi Pb-Zn deposit in Huidong, Sichuan (dissertation for Master degree)[D]. Supervisor: Mao X D. Chengdu: Chengdu University of Technology. 69p(in Chinese with English abstract).

Luo K, Zhou J X, Huang Z L, Caulfield J, Zhao J X, Feng Y X and Ouyang H G. 2020. New insights into the evolution of Mississippi Valley-Type hydrothermal system: A case study of the Wusihe Pb-Zn deposit, South China, using quartz in-situ trace elements and sulfides in situ S-Pb isotopes[J]. American Mineralogist, 105(1): 35-51.

Maanijou M, Fazel E T, Hayati S, Mohseni H and Vafaei M. 2020. Geology, fluid inclusions, C-O-S-Pb isotopes and genesis of the Ahangaran Pb-Ag (Zn) deposit, Malayer-Esfahan Metallogenic Province, western Iran[J]. Journal of Asian Earth Sciences, 195: 104339.

Machel H G, Krouse H R and Sassen R. 1995. Products and distin-

guishing criteria of bacterial and thermochemical sulfate reduction[J]. Applied Geochemistry, 10(4): 373-389.

Maréchal C and Sheppard S M F. 2002. Isotopic fractionation of Cu and Zn between chloride and nitrate solutions and malachite or smithsonite at 30℃ and 50℃ [J]. Geochimica et Cosmochimica Acta, 66: A484.

Mason T F D, Weiss D J, Chapman J B, Wilkinson J J, Tessalina S G, Spiro B, Horstwood M S A, Spratt J and Coles B J. 2005. Zn and Cu isotopic variability in the Alexandrinka volcanic-hosted massive sulphide (VHMS) ore deposit, Urals, Russia[J]. Chemical Geology, 221(3): 170-187.

Moeller K, Schoenberg R, Pedersen R B, Weiss D and Dong S. 2012. Calibration of the new certified reference materials ERM-AE633 and ERM-AE647 for copper and IRMM-3702 for zinc isotope amount ratio determinations[J]. Geostandards and Geoanalytical Research, 36(2): 177-199.

Ohmoto H and Lasaga A. 1982. Kinetics of reactions between aqueous sulfates and sulfides in hydrothermal systems[J]. Geochimica et Cosmochimica Acta, 46: 1727-1745.

Pašava J, Tornos F and Chrastný V. 2014. Zinc and sulfur isotope variation in sphalerite from carbonate-hosted zinc deposits, Cantabria, Spain[J]. Mineralium Deposita, 49(7): 797-807.

Pass H E, Cooke, D R, Davidson G, Maas R, Dipple G, Rees C, Ferreira L, Taylor C and Deyell C L. 2014. Isotope geochemistry of the northeast zone, Mount Polley Alkalic Cu-Au-Ag porphyry deposit, British Columbia: A case for carbonate assimilation[J]. Econ. Geol., 109: 859-890.

Rddad L. 2021. The genesis of the Jurassic-hosted Mississippi Valley-type Pb-Zn ore deposit, Tigrinine-Taabast district (Central High Atlas, Morocco): Insights from fluid inclusion and C-O-S-Pb isotope studies[J]. Journal of African Earth Sciences, 174:104071.

Ren S L, Li Y H, Zeng P S, Qiu W L, Fan C F and Hu G Y. 2018. Efect of sulfate evaporate salt layer in mineralization of the Huize and Maoping lead-zinc deposits in Yunnan: Evidence from sulfur isotope[J]. Acta Geologica Sinica, 92(5):1041-1055 (in Chinese with English abstract).

Ren T, Zhou J X, Wang D, Yang G S and Lv C L. 2019. Trace elemental and S-Pb isotopic geochemistry of Fule Pb-Zn deposit, NE Yunnan Province[J]. Acta Petrologica Sinica, 35(11): 3493-3505 (in Chinese with English abstract).

Shan L, Zheng Y Y, Xu R K, Cao L, Zhang Y L, Lian Y L and Li Y H. 2009. Review on sulfur isotopic tracing and hydrothermal metallogenesis[J]. Geology and Resources, 18(3): 197-203(in Chinese with English abstract).

Shellnutt J G. 2014. The Emeishan large igneous province: A synthesis[J]. Geoscience Frontiers, 5(3):369-394.

Shellnutt J G, Pham T T, Denyszyn S W, Yeh M W and Tran T A. 2020. Magmatic duration of the Emeishan large igneous province: Insight from northern Vietnam[J]. Geology, 48(5):457-461.

Sun W D, Wei G J, Zhang Z F, Ding X and Ling M X. 2012. Research status and advance in isotope geochemistry[J]. Buletin of Mineralogy, Petrology and Geochemistry, 31(6): 560-564(in Chinese with English abstract).

Tan S C, Zhou J X, Luo K, Xiang Z Z, He X H and Zhang Y H. 2019. The sources of ore-forming elements of the Maoping large-scale Pb-Zn deposit, Yunnan Province[J]. Acta Petrologica Sinica, 35 (11): 3461-3476(in Chinese with English abstract).

Tan S C, Zhou J X, Zhou M F and Ye L. 2019. In-situ S and Pb isotope constraints on an evolving hydrothermal system, Tianbaoshan Pb-Zn-(Cu) deposit in South China[J]. Ore Geology Reviews, 115: 103177.

Wang H, Wang J B, Zhu X Y, Li Y S, Zhen S M, Sun H R, Cheng X Y, Han Y, Sun Z J and Jiang B B. 2018. Genesis of the Dalingzi Pb-Zn deposit in the western margin of Yangtze Plate: Constraints from fluid inclusions and isotopic evidence[J]. Geotectonica et Metallogenia, 42(4): 681-698(in Chinese with English abstract).

Wang J, Yao C L and Li Z L. 2019. Deep structure in the Emeishan large igneous province revealed by inversion of magnetic anomalies[J]. Chinese Journal of Geophysics, 62(4): 1394-1404(in Chinese with English abstract).

Wang L J, Mi M, Zhou J X and Luo K. 2018. New constraints on the origin of the Maozu carbonate-hosted epigenetic Zn-Pb deposit in NE Yunnan Province, SW China[J]. Ore Geology Reviews, 101: 578-594.

Wang L, Han R S, Zhang Y and Wang J S. 2016. Sulfur isotopic geochemistry of the Huize Pb-Zn ore field in Yunnan Province[J]. Bulletin of Mineralogy, Petrology and Geochemistry, 35(6): 1248-1257(in Chinese with English abstract).

Wang Y F and Yang H M. 2016. Sulfur isotope tracing of ore-forming hydrothermal fluid for metallic sulfide deposit[J]. Advances in Earth Science, 31(6): 595-602(in Chinese with English abstract).

Wang Z W, Yuan W and Chen J B. 2015. Zn stable isotope geochemistry: A review[J]. Earth Science Frontiers, 22(5):84-93(in Chinese with English abstract).

Wei C, Ye L, Li Z L, Hu Y S, Huang Z L, Liu Y P and Wang H Y. 2020. Metal sources and ore genesis of the Wusihe Pb-Zn deposit in Sichuan, China: New evidence from in-situ S and Pb isotopes[J]. Acta Petrologica Sinica, 36(12): 3783-3796.

Wei C, Huang Z L, Ye L, Hu Y S, Santosh M, Wu T, He L L, Zhang J W, He Z W, Xiang Z Z, Chen D, Zhu C W and Jin Z G. 2021a. Genesis of carbonate- hosted Zn-Pb deposits in the Late Indosinian thrust and fold systems: An example of the newly discovered giant Zhugongtang deposit, South China[J]. Journal of Asian Earth Sciences, 220: 104914.

Wei C, Ye L, Huang Z L, Hu Y S and Wang H Y. 2021b. In situ trace elements and S isotope systematics for growth zoning in sphalerite from MVT deposits: A case study of Nayongzhi, South China[J]. Mineralogical Magazine, 85(3): 364-378.

Wilkinson J J, Weiss D J, Mason T F D and Coles B J. 2005. Zinc isotope variation in hydrothermal systems: Preliminary evidence from the Irish Midlands ore field[J]. Econ. Geol., 100(3): 583-590.

Wu T, Huang Z L, He Y F, Yang M, Fan H F, Wei C, Ye L, Hu Y S and

Lai C. 2021. Metal source and ore-forming process of the Maoping carbonate-hosted Pb-Zn deposit in Yunnan, SW China: Evidence from deposit geology and sphalerite Pb-Zn-Cd isotopes[J]. Ore Geology Reviews, 135:104214.

Wu Y D, Wang Z Q, Luo J H, Cheng J X, Zhang Y L and Wang S D. 2016. Geochemical characteristics and metallogenic mechanism analysis of Huodehong lead-zinc deposit, Northeast Yunnan Province[J]. Mineral Deposits, 35(5): 1084-1098(in Chinese with English abstract).

Wu Y. 2013. The age and ore-forming process of MVT deposits in the boundary area of Sichuan-Yunnan-Guizhou Provinces, Southwest China (dissertation for Doctor degree)[D]. Supervisor: Mao J W and Zhang C Q. Beijing: China University of Geosciences. 167p (in Chinese with English abstract).

Xiang Z Z, Zhou J X and Luo K. 2020. New insights into the multi-layer metallogenesis of carbonated-hosted epigenetic Pb-Zn deposits: A case study of the Maoping Pb-Zn deposit, South China[J]. Ore Geology Reviews, 122:103538.

Xie J R. 1941. Discussion on metallogeny[J]. Geological Review, 6 (Z1):1-42(in Chinese with English abstract).

Xu C, Zhong H, Hu R Z, Wen H J, Zhu W G, Bai Z J, Fan H F, Li F F and Zhou T. 2020. Sources and ore-forming fluid pathways of carbonate-hosted Pb-Zn deposits in Southwest China: Implications of Pb-Zn-S-Cd isotopic compositions[J]. Mineralium Deposita, 55 (3): 491-513.

Yang Q. 2021. Study on mineralization of lead-zinc deposits in northeastern Yunnan and northwestern Guizhou Province, China (dissertation for Master degree)[D]. Supervisor: Zhang J. Wuhan: China University of Geosciences. 183p(in Chinese with English abstract).

Yang X Y, Zhou J X, An Q, Ren H F, Xv L, Lu M D and Wu C J. 2018. Formation mechanism of reduced S in the Nayongzhi Pb-Zn deposit, Guizhou Province, China: Constraint from the NanoSIMS in-situ S isotopes[J]. Acta Mineralogica Sinica, 38(6): 593-599 (in Chinese with English abstract).

Yuan B, Mao J W, Yan X H, Wu Y, Zhang F and Zhao L L. 2014. Sources of metallogenic materials and metallogenic mechanism of Daliangzi ore field in Sichuan Province: Constraints from geochemistry of S, C, H, O, Sr isotope and trace element in sphalerite[J]. Acta Petrologica Sinica, 30(1): 209-220(in Chinese with English abstract).

Zartman R E and Doe B R. 1981. Plumbotectonics—the model[J]. Tectonophysics, 75(1): 135-162.

Zhang C Q. 2005. Distribution, characteristics and genesis of Mississippi Valley-type lead-zinc deposits in the triangle area of Sichuan-Yunnan-Guizhou Provinces (dissertation for Master degree)[D]. Supervisor: Mao J W. Beijing: China University of Geosciences. 94p(in Chinese with English abstract).

Zhang C Q, Mao J W, Wu S P, Li H M, Liu F, Guo J H and Gao D R. 2005. Distribution, characteristics and genesis of Mississippi Valley-Type lead-zinc deposits in Sichuan-Yunnan-Guizhou area[J]. Mineral Deposits, 24(3): 336-348(in Chinese with English abstract).

Zhang H J, Fan H F, Xiao C Y, Wen H J, Ye L, Huang Z L, Zhou J X and Guo Q J. 2019a. The mixing of multi-source fluids in the Wusihe Zn-Pb ore deposit in Sichuan Province, southwestern China[J]. Acta Geochimica, 38(5): 642-653.

Zhang H J, Xiao C Y, Wen H J, Zhu X K, Ye L, Huang Z L, Zhou J X and Fan H F. 2019b. Homogeneous Zn isotopic compositions in the Maozu Zn-Pb ore deposit in Yunnan Province, southwestern China[J]. Ore Geology Reviews, 109: 1-10.

Zhang W J. 1984. Discussion on genesis and forming law of Pb-Zn deposits in Northeast Yunnan[J]. Geology and Prospecting, (7): 11-16(in Chinese with English abstract).

Zhang Y X, Wu Y, Tian G, Shen L, Zhou Y M, Dong W W, Zeng R, Yang X C and Zhang C Q. 2014. Mineralization age and the source of ore-forming material at Lehong Pb-Zn deposit, Yunnan Province: Constraints from Rb-Sr and S isotopes system[J]. Acta Mieralogica Sinica, 34(3): 305-311(in Chinese with English abstract).

Zhou J X, Huang Z L and Yan Z F. 2013a. The origin of the Maozu carbonate-hosted Pb-Zn deposit, Southwest China: Constrained by C-O-S-Pb isotopic compositions and Sm-Nd isotopic age[J]. Journal of Asian Earth Sciences, 73: 39-47.

Zhou J X, Huang Z L, Gao J G and Wang T. 2012. Sources of ore-forming metals and fluids, and mechanism of mineralization, Maozu large carbonate-hosted lead-zinc deposit, Northeast Yunnan Province[J]. Mineralogy and Petrology, 32(03): 62-69 (in Chinese with English abstract).

Zhou J X, Huang Z L, Lv Z C, Zhu X K, Gao J G and Mirnejad H. 2014a. Geology, isotope geochemistry and ore genesis of the Shanshulin carbonate-hosted Pb-Zn deposit, Southwest China[J]. Ore Geology Reviews, 63:209-225.

Zhou J X, Huang Z L, Ye L, Bao Z W, Liu Y and Xia Y. 2015. Research progress of the mineralization of carbonate-hosted Pb-Zn deposits in the Sichuan-Yunnan-Guizhou Pb-Zn metallogenic province, Southwest China[J]. Acta Geologica Sinica(English Edition), 89(1): 307-308.

Zhou J X, Huang Z L, Zhou M F, Li X B and Jin Z G. 2013b. Constraints of C-O-S-Pb isotope compositions and Rb-Sr isotopic age on the origin of the Tianqiao carbonate-hosted Pb-Zn deposit, SW China[J]. Ore Geology Reviews, 53:77-92.

Zhou J X, Huang Z L, Zhou M F, Zhu X K and Muchez P. 2014b. Zinc, sulfur and lead isotopic variations in carbonate-hosted Pb-Zn sulfide deposits, Southwest China[J]. Ore Geology Reviews, 58: 41-54.

Zhou J X, Luo K, Wang X C, Wilde S A, Wu T, Huang Z L, Cui Y L and Zhao J X. 2018a. Ore genesis of the Fule Pb-Zn deposit and its relationship with the Emeishan Large Igneous Province: Evidence from mineralogy, bulk C-O-S and in situ S-Pb isotopes[J]. Gondwana Research, 54: 161-179.

Zhou J X, Wang X C, Wilde S A, Luo K, Huang Z L, Wu T and Jin Z

G. 2018b. New 1Nayongzhi in South China, using field data, fluid compositions, and in situ S- Pb isotopes[J]. American Mineralogist,103(1): 91-108.

Zhu B Q. 1998. Theory and application isotope system in the earth science: Crust mantle evolution of China[M]. Beijing: Science Press. 330p( in Chinese).

Zhu C W, Liao S L, Wang W, Zhang Y X, Yang T, Fan H F and Wen H J. 2018. Variations in Zn and S isotope chemistry of sedimentary sphalerite, Wusihe Zn-Pb deposit, Sichuan Province, China[J]. Ore Geology Reviews, 95: 639-648.

Zhu C W, Wen H J, Zhang Y X and Fan H F. 2016. Cadmium and sulfur isotopic compositions of the Tianbaoshan Zn-Pb-Cd deposit, Sichuan Province, China[J]. Ore Geology Reviews, 76: 152-162.

Zhu C W, Wang J, Zhang J W, Chen X C, Fan H F, Zhang Y X, Yang T and Wen H J. 2020. Isotope geochemistry of Zn, Pb and S in the Ediacaran strata hosted Zn-Pb deposits in Southwest China[J]. Ore Geology Reviews, 117:103274.

## 附中文参考文献

付绍洪 . 2004. 扬子地块西南缘铅锌成矿作用与分散元素镉镓锗富集规律(硕士学位论文)[D]. 导师: 顾雪祥 . 成都: 成都理工大学 . 94 页 .

韩润生, 陈进, 黄智龙, 马德云, 薛传东, 李元, 邹海俊, 李勃, 胡煜昭, 马更生, 黄德镛, 王学琨 . 2006. 构造成矿动力学及隐伏矿定位预测——以云南会泽超大型铅锌(银, 锗)矿床为例[M]. 北京: 科学出版社 . 239 页 .

韩润生, 胡煜昭, 王学琨, Hou B H, 黄智龙, 陈进, 王峰, 吴鹏, 李波, 王洪江, 董英, 雷丽 . 2012. 滇东北富锗银铅锌多金属矿集区矿床模型[J]. 地质学报, 86(02):280-294.

何承真, 肖朝益, 温汉捷, 周汀, 朱传威, 樊海峰 . 2016. 四川天宝山铅锌矿床的锌-硫同位素组成及成矿物质来源[J]. 岩石学报, 32(11):3394-3406.

何承真 . 2017. 四川天宝山铅锌矿床 Zn-S 同位素地球化学特征及成矿物质来源(硕士学位论文)[D]. 导师: 樊海峰, 卢定彪 . 贵阳: 中国科学院地球化学研究所 . 65 页 .

胡瑞忠, 陈伟, 毕献武, 付山岭, 尹润生, 肖加飞 . 2020. 扬子克拉通前寒武纪基底对中生代大面积低温成矿的制约[J]. 地学前缘, 27(02):137-150.

黄智龙, 陈进, 刘丛强, 韩润生, 李文博, 赵德顺, 高德荣, 冯志宏 . 2001. 峨眉山玄武岩与铅锌矿床成矿关系初探——以云南会泽铅锌矿床为例[J]. 矿物学报, 21(4): 681-688.

黄智龙, 李文博, 张振亮, 韩润生, 陈进 . 2004. 云南会泽超大型铅锌矿床成因研究中的几个问题[J]. 矿物学报, 24(02):105-111.

金灿海, 张玙, 沈战武, 张达 . 2016. 滇东北火德红铅锌矿矿床地质特征及成矿物质来源[J]. 矿物岩石, 36(4): 50-56.

金中国, 周家喜, 黄智龙, 罗开, 高建国, 彭松, 王兵, 陈兴龙 . 2016. 贵州普定纳雍枝铅锌矿矿床成因: S 和原位 Pb 同位素证据[J]. 岩石学报, 32(11): 3441-3455.

孔志岗, 吴越, 张锋, 张长青, 孟旭阳 . 2018. 川滇黔地区典型铅锌矿床成矿物质来源分析: 来自 S-Pb 同位素证据[J]. 地学前缘, 25(1): 125-137.

李波 . 2008. 云南巧家松梁铅锌矿床地质特征及构造地球化学异常模式(硕士学位论文)[D]. 导师: 韩润生, 顾晓春 . 昆明: 昆明理工大学 . 116 页 .

李波 . 2010. 滇东北地区会泽、松梁铅锌矿床流体地球化学与构造地球化学研究(博士学位论文)[D]. 导师: 韩润生, 顾晓春 . 昆明: 昆明理工大学 . 194 页 .

李波, 顾晓春, 韩润生, 文书明, 徐国端, 曹宇, 吴昊, 邹国富, 盛蕊 . 2012. 滇东北巧家县松梁铅锌矿床地质特征及成矿条件分析[J]. 矿产与地质, 26(1): 13-18+67.

李波, 韩润生, 文书明, 盛蕊, 邱文龙, 唐果 . 2014. 滇东北巧家松梁铅锌矿床构造特征及构造地球化学[J]. 大地构造与成矿学, 38(4): 855-865.

李文博, 黄智龙, 陈进, 许成, 管涛, 尹牡丹 . 2004. 云南会泽超大型铅锌矿床硫同位素和稀土元素地球化学研究[J]. 地质学报, (4): 507-518.

李文博, 黄智龙, 张冠 . 2006. 云南会泽铅锌矿田成矿物质来源: Pb、S、C、H、O、Sr 同位素制约[J]. 岩石学报, 22(10): 2567-2580.

李延河 . 2020. "同位素分析新技术与地质应用研究新进展"专辑特邀主编寄语[J]. 地球学报, 41(5): 583-589.

廖文 . 1984. 滇东、黔西铅锌金属区硫、铅同位素组成特征与成矿模式探讨[J]. 地质与勘探, (1): 2-6.

刘志鹏 . 2016. 四川会东大梁子铅锌矿床稳定同位素地球化学研究(硕士学位论文)[D]. 导师: 毛晓冬 . 成都:成都理工大学 . 69 页 .

任顺利, 李延河, 曾普胜, 邱文龙, 范昌福, 胡古月 . 2018. 膏盐层在云南会泽和毛坪铅锌矿成矿中的作用: 硫同位素证据[J]. 地质学报, 92(5): 1041-1055.

任涛, 周家喜, 王蝶, 杨光树, 吕昶良 . 2019. 滇东北富乐铅锌矿床微量元素和 S-Pb 同位素地球化学研究[J]. 岩石学报, 35(11): 3493-3505.

陕亮, 郑有业, 许荣科, 曹亮, 张雨莲, 连永牢, 李闫华 . 2009. 硫同位素示踪与热液成矿作用研究[J]. 地质与资源, 18(3): 197-203.

孙卫东, 韦刚健, 张兆峰, 丁兴, 凌明星 . 2012. 同位素地球化学发展趋势[J]. 矿物岩石地球化学通报, 31(6): 560-564.

谈树成, 周家喜, 罗开, 向震中, 何小虎, 张亚辉 . 2019. 云南毛坪大型铅锌矿床成矿物质来源: 原位 S 和 Pb 同位素制约[J]. 岩石学报, 35(11): 3461-3476.

王海, 王京彬, 祝新友, 李永胜, 甄世民, 孙海瑞, 程细音, 韩英, 孙紫坚, 蒋斌斌 . 2018. 扬子地台西缘大梁子铅锌矿床成因: 流体包裹体及同位素地球化学约束[J]. 大地构造与成矿学, 42(4): 681-698.

王婕, 姚长利, 李泽林 . 2019. 磁异常揭示的峨眉山大火成岩省的深部结构[J]. 地球物理学报, 62(4): 1394-1404.

王磊, 韩润生, 张艳, 王加昇 . 2016. 云南会泽铅锌矿田硫同位素研究[J]. 矿物岩石地球化学通报, 35(6):1248-1257.

王云峰, 杨红梅 . 2016. 金属硫化物矿床的成矿热液硫同位素示踪[J]. 地球科学进展, 31(6): 595-602.

王中伟, 袁玮, 陈玖斌 . 2015. 锌稳定同位素地球化学综述[J]. 地学前缘, 22(5): 84-93.

吴越 . 2013. 川滇黔地区 MVT 铅锌矿床大规模成矿作用的时代与机

制(博士学位论文)[D]. 导师: 毛景文, 张长青 . 北京: 中国地质大学 . 167 页 .

武昱东, 王宗起, 罗金海, 程家孝, 张英利, 王师迪 . 2016. 滇东北火德红铅锌矿床地球化学特征与成矿机制分析[J]. 矿床地质, 35(5): 1084-1098.

谢家荣 . 1941. 云南矿产概论[J]. 地质论评, 6(Z1): 1-42.

杨清 . 2021. 滇东北-黔西北地区铅锌矿床成矿作用研究(博士学位论文)[D]. 导师: 张均 . 武汉: 中国地质大学 . 183 页 .

杨兴玉, 周家喜, 安琦, 任厚州, 徐磊, 卢贸达, 吴才进 . 2018. 贵州纳雍枝铅锌矿床还原 S 的形成机制: NanoSIMS 原位 S 同位素约束[J]. 矿物学报, 38(6): 593-599.

袁波, 毛景文, 闫兴虎, 吴越, 张锋, 赵亮亮 . 2014. 四川大梁子铅锌矿成矿物质来源与成矿机制: 硫、碳、氢、氧、锶同位素及闪锌矿微量元素制约[J]. 岩石学报, 30(1): 209-220.

张位及 . 1984. 试论滇东北铅锌矿床的沉积成因和成矿规律[J]. 地质与勘探, (7): 11-16.

张云新, 吴越, 田广, 申亮, 周云满, 董文伟, 曾荣, 杨兴潮, 张长青 . 2014. 云南乐红铅锌矿床成矿时代与成矿物质来源: Rb-Sr 和 S 同位素制约[J]. 矿物学报, 34(3): 305-311.

张长青 . 2005. 川滇黔地区 MVT 铅锌矿床分布、特征及成因研究(硕士学位论文)[D]. 导师: 毛景文 . 北京:中国地质大学 . 94 页 .

张长青, 毛景文, 吴锁平, 李厚民, 刘峰, 郭保健, 高德荣 . 2005. 川滇黔地区 MVT 铅锌矿床分布、特征及成因[J]. 矿床地质, 24(3): 336-348.

周家喜, 黄智龙, 高建国, 王涛 . 2012. 滇东北茂租大型铅锌矿床成矿物质来源及成矿机制[J]. 矿物岩石, 32(3): 62-69.

朱炳泉 . 1998. 地球科学中同位素体系理论与应用: 兼论中国大陆壳幔演化[M]. 北京: 科学出版社 . 330 页 .